Marine Pollution Bulletin 168 (2021) 112409

Contents lists available at ScienceDirect

Marine Pollution Bulletin

journal homepage: www.elsevier.com/locate/marpolbul

The effect of natural and anthropogenic nutrient and sediment loads on coral oxidative stress on runoff-exposed reefs

Mark E. Baird [a,*], Mathieu Mongin [a], Farhan Rizwi [a], Line K. Bay [b], Neal E. Cantin [b], Luke A. Morris [b,c,d], Jennifer Skerratt [a]

[a] CSIRO Oceans and Atmosphere, Hobart 7001, Australia
[b] Australian Institute of Marine Science, Townsville 4810, Australia
[c] AIMS@JCU, Australian Institute of Marine Science, College of Science and Engineering, Townsville 4811, Australia
[d] College of Science and Engineering, James Cook University, Townsville 4811, Australia

ARTICLE INFO

Keywords:
Symbiodiniaceae
Mass bleaching
Biogeochemical model
Climate change
Coral mortality
Great Barrier Reef

ABSTRACT

Recently, corals on the Great Barrier (GBR) have suffered mass bleaching. The link between ocean warming and coral bleaching is understood to be due to temperature-dependence of complex physiological processes in the coral host and algal symbiont. Here we use a coupled catchment-hydrodynamic-biogeochemical model, with detailed zooxanthellae photophysiology including photoadaptation, photoacclimation and reactive oxygen build-up, to investigate whether natural and anthropogenic catchment loads impact on coral bleaching on the GBR. For the wet season of 2017, simulations show the cross-shelf water quality gradient, driven by both natural and anthropogenic loads, generated a contrasting zooxanthellae physiological state on inshore versus mid-shelf reefs. The relatively small catchment flows and loads delivered during 2017, however, generated small river plumes with limited impact on water quality. Simulations show the removal of the anthropogenic fraction of the catchment loads delivered in 2017 would have had a negligible impact on bleaching rates.

1. Introduction

Coral bleaching is the expulsion from the coral host of the photosynthetic unicellular symbionts (of the family Symbiodiniaceae (LaJeunesse et al., 2018) and referred to here generically as zooxanthellae). A number of environmental stressors can lead to bleaching such as periods of anomalously-high temperature, prolonged high light intensity or low salinity exposure. The mass bleaching events on the Great Barrier (GBR) over the last two decades have coincided with periods of prolonged heat stress (Hoegh-Guldberg, 1999; Hughes et al., 2018b). The physiological process in the zooxanthellae that is considered most responsible for bleaching during thermal stress events is the temperature-mediated, light-driven build-up of reactive oxygen stress in zooxanthellae (Suggett et al., 2008).

The response of zooxanthellae to environmental stress involves a complicated set of interactions. Within the zooxanthella cell photosystem, photoadaptation and photoinhibition processes respond to changes in light on the scale of minutes to days (Falkowski and Raven, 1997). The coral host and their algal symbionts exchange organic compounds, a phenomenon that is vital to the ecological and evolutionary success of corals (Yonge, 1930; Muscatine and Porter, 1977), resulting in varying cell densities over periods of weeks. At the time scale of seasons to years, ecological process drive dynamical processes. For example, coral populations interact with other coral species, as well as predators such as starfish, undergoing population cycles (Hock et al., 2017; Condie et al., 2018), adapt through relative survival of hardier species (Hughes et al., 2018a) and building habitats that can last for millennia (Maxwell, 1968).

While the link between light, temperature and bleaching is clear (Skirving et al., 2018), it has also been proposed that anthropogenic nutrient loads increase the vulnerability of corals to thermal bleaching (Wooldridge, 2009, 2020; Wiedenmann et al., 2013; Morris et al., 2019; Rädecker et al., 2021). If such a link between nutrient availability and bleaching is confirmed, then catchment protection, one of the key existing environmental management strategies on the GBR (Brodie and Waterhouse, 2012), and other reef systems (Lapointe et al., 2010; Donovan et al., 2020), will take on an even greater importance.

Changing sediment loads could also impact on bleaching. The

* Corresponding author.
E-mail address: mark.baird@csiro.au (M.E. Baird).

https://doi.org/10.1016/j.marpolbul.2021.112409
Received 11 September 2020; Received in revised form 16 April 2021; Accepted 17 April 2021

negative effects of sediments on coral health through smothering coral tissue and shading the photosynthetic symbionts are well known (Rogers, 1990). Conversely, increased turbidity has a protective effect during bleaching by reducing stressful light conditions (Sully and van Woesik, 2020; Oxenford and Vallès, 2016). As bleaching is potentially impacted by both nutrient and sediment loads, the effect of catchment management strategies on nutrients and sediments needs to be considered simultaneously.

For catchment-derived nutrients and sediments to have a significant impact on coral bleaching in the GBR, they must be transported to the reef site, and then be in sufficient concentrations to impact on the zooxanthellae physiology and/or coral processes. The delivery of nutrients to a reef site involves a complex interaction of time-varying physical factors such as large scale circulation and local winds, tides, and river discharges (see analysis by Wolff et al. (2018), Bainbridge et al. (2018)). River discharges on the GBR also exhibit large interannual variability (Devlin et al., 2013), driven by climatic cycles such as El Niño — Southern Oscillation (ENSO). Until 2020, the most significant bleaching events on the GBR (1998, 2002, 2016 and 2017) have all occurred in low rainfall years.

During the transport of a particle or nutrient-laden water parcel to a reef site, biogeochemical transformations occur in both the water column and sediments, such as nutrient uptake by microalgae, seagrass and macroalgae, absorption and desorption onto particles, denitrification and remineralisation (Bainbridge et al., 2018). These processes change the nature of the pollutant loads that impact corals (Devlin et al., 2015). Furthermore, catchment-derived loads mix with nutrients and sediments from locally-generated in-water processes including nitrogen fixation, upwelling and resuspension. Thus, disentangling the impact of catchment-derived pollutants on coral bleaching across the GBR is a challenge beyond our present observational capabilities.

As an initial step to relating Dissolved Inorganic Nitrogen (DIN, abbreviations defined in Table 1) loads to environmental conditions above reefs, Wolff et al. (2018) developed correlations between loads and DIN concentrations along plume transects, and then applied these relationships to quantify the exposure of individual reefs to catchment loads. The Wolff et al. (2018) study was undertaken during the wet years of 2010/11 and 2011/12, and found in 2011 some reefs were exposed to river nutrients for the entire wet seasons, while others had more moderate exposure. The reefs that are considered in this manuscript, Otter, Havannah and Pandora, were exposed to 67 and 18, 101 and 37, and 100 and 35 days respectively in 2010/11 and 2011/12. While the modelling approach in Wolff et al. (2018) coarsely disentangled dilution from biogeochemical transformations within the plumes, it relied heavily on correlations between biogeochemical observations within a limited number of plumes and river discharge along the entire GBR.

Table 1
Abbreviations and mathematical symbols. For more mathematical symbols used in equations see Baird et al. (2018).

C:N:P	Carbon:nitrogen:phosphorus
DIN	Dissolved Inorganic Nitrogen
DON	Dissolved Organic Nitrogen
PN	Particulate Nitrogen
DIP	Dissolved Inorganic Phosphorus
DOP	Dissolved Organic Phosphorus
PIP	Particulate Inorganic Phosphorus
TSS	Total Suspended Sediments
ROS	Reactive Oxygen Species
POM	Particulate Organic Matter
Q_x	Fraction of reaction centres in state, x x = ox (oxidised), red (reduced), in (inhibited)
a_{ox}*	Activity of the RuBisCo enzyme (0 inactive; 1 fully active)
R_X*	Normalised reserves of X = C, N, P (0 empty; 1 full)
T_{clim}	Climatological maximum summertime temperature
Chl	Chlorophyll
X_h	Heat dissipating xanthophyll pigment (diatoxanthin)
X_p	Photosynthetic xanthophyll pigment (diadinoxanthin)
RuBisCO	Ribulose-1,5-bisphosphate carboxylase/oxygenase
PAR	Photosynthetically available radiation
HPLC	High-performance liquid chromatography
ENSO	El Nino — Southern Oscillation
RECOM	RElocatable Coastal Ocean Model
GBR	Great Barrier Reef
AIMS	Australian Institute of Marine Sciences
CSIRO	Commonwealth Scientific Industrial Research Organisation

A large, multi-agency collaboration has developed the eReefs coupled hydrodynamic, sediment and biogeochemical model that simulates at multiple scales the environmental conditions of the GBR (Schiller et al., 2014; Steven et al., 2019). The project provides ~1 and ~4 km resolution hindcast and near real time simulations of hydrodynamic and biogeochemical quantities (www.ereefs.info). The models provide skillful predictions of the drivers of coral processes such as temperature, spectrally-resolved seabed light intensity, and water column concentrations of dissolved inorganic nutrients and particulate organic matter across the entire length of the GBR from 2011 to present (Skerratt et al., 2019). Furthermore, the eReefs project includes a semi-automated model generation that allows many high-resolution models to be nested within the 1 km regional hindcast (RECOM — RElocatable Coastal Ocean Model).

The coupled hydrodynamic, sediment and biogeochemical model was forced with estimates of catchment loads using the GBR Dynamic SedNet catchment model that informs land management in the GBR catchments (Waterhouse et al., 2018; Baird et al., in press). GBR Dynamic SedNet is a customised version of the SOURCE catchment model (Ellis, 2018), and has been configured to provide estimates of natural and anthropogenic basin-specific loads of dissolved inorganic, dissolved organic and particulate constituents of both nitrogen and phosphorus (DIN, DON, PN, DIP, DOP, and PP respectively), as well as sediment loads. By forcing the marine model using GBR Dynamic SedNet loads we can directly link feasible catchment load reductions with the changes in concentrations of dissolved and particulate nutrients, as well as water clarity, at the reef sites where the coral bleaching processes occur.

In order to capture the dynamics of bleaching on the GBR, a sophisticated coral physiological model was developed and implemented in the eReefs modelling system (Baird et al., 2018). The model is based on a mechanistic description of the coral-symbiont relationship that considers temperature-mediated build-up of reactive oxygen species due to excess light leading to zooxanthellae expulsion. The model explicitly represents the coral host biomass, as well as zooxanthellae biomass, intracellular pigment concentration, nutrient status, and the dynamics of photosynthetic reaction centres and the xanthophyll cycle. Photophysiological processes represented include photoadaptation, xanthophyll cycle dynamics, and reaction centre state transitions. Reactive oxygen build-up depends on light, because reactive oxygen is generated by unutilised photons, and temperature, as warmer temperatures inhibit the productive use of absorbed photons for photosynthesis, leaving more unused, or excess, photons.

In this study, we limit our analysis to the effect of catchment loads through transport in river plumes, ocean circulation and biogeochemical transformations on reactive oxygen build-up. This narrow scope is necessary, as the model simulations do not explicitly represent many of the interactions between water quality and coral health that may affecting the bleaching rate, and, in particular, the rate of mortality following bleaching. Thus, we emphasise model outputs of zooxanthellae physiological status such as cellular content of reactive oxygen species, as an indicator of bleaching processes, rather than ecological coral health measures such as coral cover or coral diversity. Our analysis of the effect of catchment loads is also based on loads delivered within one wet season, in this case 2017. The computational expense of running the highly-resolved, complex model means that we are only able to have simulations of one season duration. To be explicit, this means that our simulations will investigate the effect of catchment loads delivered in the summer of 2016/17 on zooxanthellae physiology in 2017. Therefore, we do not consider the effect of catchment loads delivered prior to

Dec 1, 2016 on coral host — zooxanthellae physiology in 2017. Finally, in addition to considering present day loads, we simulate the natural loads, defined as the estimated loads without the many alterations in catchment vegetation which have occurred since 1850. By considering the difference between present and natural loads, this study is able to quantify the effect of anthropogenic loads delivered since Dec 1, 2016 on coral bleaching in 2017.

In this paper we concentrate on the physiological response of zooxanthellae to catchment loads of nutrients and suspended sediments on five reefs in the central GBR. First we determine the end-of-catchment natural and present day loads using the GBR Dynamic SedNet model. Then we calculate the river footprints of the Mulgrave, Johnstone, Herbert, Tully and Burdekin rivers at the chosen reef sites. Finally, we quantify the response of the zooxanthellae photosystem (photo-adaptation, xanthophyll cycle dynamics, and reaction centre state transitions) at individual sites and differing depths exposed to the present day and natural catchment loads. The difference between the two load scenarios is an estimate of the impact of anthropogenic nutrient and sediment loads on reactive oxygen stress in zooxanthellae on runoff-exposed reefs, and represents the maximum mitigating effect that catchment repair could have had on coral bleaching in 2017.

2. Model description

2.1. Coral bleaching model

A model of coral host-symbiont interactions, with a particularly-detailed representation of the zooxanthellae photosystem, has been integrated into the eReefs coupled hydrodynamic–biogeochemical model. A mathematical description of the coral model is given in Baird et al. (2018), including the parameter values used for the simulations in this paper. The focus of the analysis in this paper is the zooxanthellae photosystem. Here we will provide a detailed, but qualitative, description of the model's zooxanthellae photosystem as represented in Fig. 1.

The model of coral host-symbiont interactions is process-based. That is, the model calculates the rates of change of variables describing the population dynamics and physiological state of the corals using environmental conditions such as seabed temperature, nutrient concentrations and light levels. These environmental conditions are predicted by the coupled hydrodynamic-biogeochemical model. The model calculates rates such as light absorption and growth rate of individual zooxanthella cells. The rates of change of variables are added to the present state to provide the prediction of the state at the next time step. In each model pixel, the rates and states of identical individual cells are multiplied by the number of cells per unit area to provide the rates and abundance in the spatially-resolved model.

The zooxanthella cells are represented as 5 μm radius spheres packed in two horizontal layers of the coral polyp. Within each cell is a light harvesting complex consisting of a set of pigments absorbing photons and passing these through a chlorophyll-*a* molecule on to a reaction centre (Fig. 1). The reaction centre changes state based on the supply of photons from the light-harvesting complex and their ultimate fate as either the energy source for fixing carbon, the transition of reaction states, or the production of reactive oxygen species (Fig. 1). Each zooxanthella cell contains of the order of 10^9 reaction centres with ~500 chlorophyll-*a* molecules per reaction centre (calculated from data in Suggett et al. (2008)). First we will consider the light-harvesting complex, and then the reaction centre complex.

2.1.1. Light-harvesting complex

The light-harvesting complex in the model includes five photosynthetic pigments (chlorophyll *a*, peridinin, β-carotene, chlorophyll c_2, and the photosynthetic xanthophyll diadinoxanthin, X_p), chosen because they are the dominant absorbing pigments in zooxanthellae as determined from HPLC concentration estimates (Clementson and Wojtasiewicz, 2019b) and mass-specific absorption coefficients (Clementson and Wojtasiewicz, 2019a).

The rate of photon absorption for photosynthesis is calculated by summing the mass-specific absorption rate multiplied by the cellular concentration of each photosynthetic pigments, and then applying this per unit length measure to the geometrically-calculated, spatially-integrated pathlength of light through the 5 μm radius cell, following Duysens (1956). This calculation gives the absorption-cross section of cell. The absorption-cross section, determined across the photosynthetically available wavelengths, is then multiplied by the spectrally-resolved seabed downwelling irradiance to give the quantity of photons absorbed. These photons are all passed onto the chlorophyll-*a* molecule, and eventually the reaction centres. Pigment synthesis, which affects the cellular concentration of pigments, occurs in set ratios between chlorophyll-*a* and the accessory pigments. The rate of pigment synthesis depends on the effectiveness that increasing pigment concentrations will have on zooxanthella growth, and is itself a function of the available fixed carbon reserves (R_C*) and the opaqueness of the cell. A more opaque cell has a diminishing benefit to adding pigment since it is already absorbing the bulk of the photons intercepted by the cell (Baird et al., 2013). An energy replete cell will also not benefit from additional pigment, so synthesis is slowed.

Finally, photoacclimation through a xanthophyll cycle is resolved.

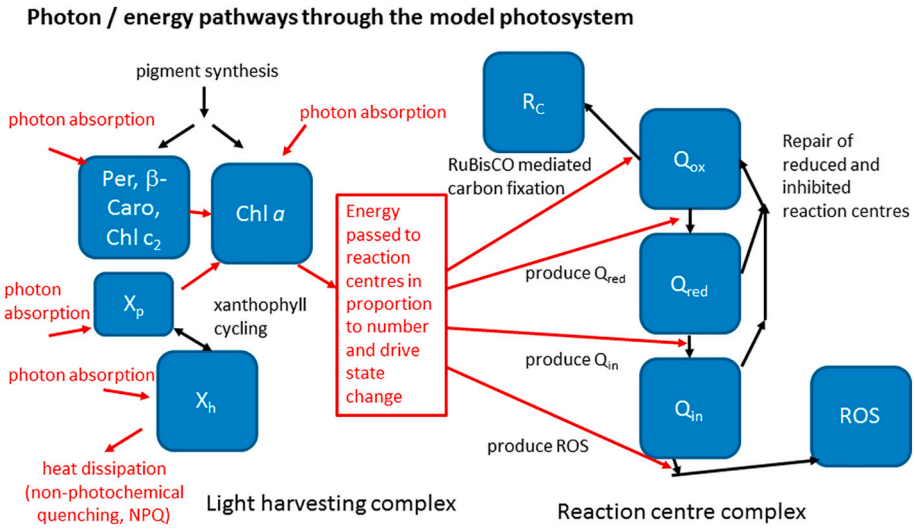

Fig. 1. Schematic showing on the left the light harvesting complex that includes photosynthetic (chlorophyll *a*, peridinin, β-carotene, chlorophyll c_2, and the photosynthetic xanthophyll diadinoxanthin, X_p) and the photoprotective (xanthophyll diatoxanthin, X_h) pigments, and includes the processes of pigment synthesis and xanthophyll cycling. On the right is the reaction centre complex that, depending on physiological state, processes photons into fixed carbon, reaction state transitions or reactive oxygen species generation. Red arrows depict fluxes of photons/electrons. Black arrows show transformations of state of either reaction centres or xanthophyll cycle pigments. (For interpretation of the references to colour in this figure legend, the reader is referred to the web version of this article.)

The model represents the switching of the photosynethic xanthophyll pigment diadinoxanthin to the heat dissipating form diatoxanthin. The total xanthophyll pigment content remains constant during switching. Diadinoxanthin switches to diatoxanthin as a function of the fraction of inactive reaction centres, with the rate of switching slowing as the transition becomes completed. With the fast switch rate used in the model, complete transition of the xanthophyll pigments can occur in less than hour.

2.1.2. Reaction centre complex

Three states of reaction centres are resolved: oxidised, reduced and inhibited. The process of photons changing reaction centre states, and the driving of carbon fixation or reactive oxygen species build-up, is stoichiometric. For example, the absorption of 10 photons leads to 1 carbon molecule being fixed or 1 reaction centre being reduced. The use of fixed stoichiometry reduces the number of empirical coefficients that are required in the model.

Up until this point in the coral model description we have not mentioned temperature inhibition, the key environmental variable mediating bleaching. At normal temperatures, most of the photons passed to reaction centres are used for carbon fixation, so they do not lead to reaction centres becoming reduced and then inhibited. However, at elevated temperatures photons cannot be productively used for carbon fixation and instead push reaction centres to a more inhibit state. The other case of reduced carbon fixation is under extreme nutrient limitation when the carbon reserves saturate because there are no nutrients to facilitate growth and therefore deplete carbon reserves. Initially the inhibition of carbon fixation transitions oxidised reaction states to reduced states. Photons absorbed by reduced reaction centres drive them to an inhibited state. And any photons absorbed by inhibited reaction centres produce reactive oxygen species. There are repair processes that return reduced and inhibited processes to an oxidised state, but these do not keep up with excess absorbed photons under bleaching conditions. Thus, the temperature-mediated inhibition of carbon fixation, combined with high photon absorption, drives increasing reactive oxygen stress.

Finally, an empirical relationship is used for the rate of zooxanthella expulsion from reactive oxygen content. For ROS concentrations up to a threshold level no expulsion occurs. Above the threshold, the expulsion rate is proportional to the above threshold concentration, up to a maximum of 1 per day per zooxanthella.

In the model, how do water column nutrient concentrations affect bleaching? As mentioned above, carbon reserves are drawn down by growth, which itself is a function of reserves of nutrients. If zooxanthellae are extremely nutrient deplete, then nutrient supply can increase growth and therefore reduce carbon reserves, reducing reactive oxygen build-up. On the other hand, increasing growth will produce greater zooxanthellae densities per coral polyp, greater absorption of photons, eventually increasing the reactive oxygen build-up per polyp. And while not emphasised above, zooxanthellae population dynamics, in combination with organic particulate feeding from water column plankton communities, also affects bleaching through control on zooxanthella population densities (Gustafsson et al., 2014; Baird et al., 2018). And as a final factor, light penetration to the seabed is also affected by plankton dynamics in the water column, itself driven by nutrient inputs and recycling.

In summary, a complex, but mechanistically-derived, model of the zooxanthellae photosystem allows for the representation of the interaction of temperature-mediated carbon fixation and water column nutrient and light levels on the coral bleaching rate. When the zooxanthellae photosystem model is combined with the coupled catchment-hydrodynamic-biogeochemical model that can predict the nutrients reaching the reefs from catchments, the influence of catchment loads on coral bleaching can be examined.

2.2. GBR Dynamic SedNet catchment model

The GBR Dynamic SedNet model (Waters et al., 2014; Waterhouse et al., 2018; McCloskey et al., 2021) was used to predict the basin-specific loads of Dissolved Inorganic Nitrogen (DIN), Dissolved Organic Nitrogen (DON), Particulate Nitrogen (PN), Dissolved Inorganic Phosphorus (DIP), Dissolved Organic Phosphorus (DOP), Particulate Inorganic Phosphorus (PIP) and Total Suspended Sediments (TSS) entering the marine model. The full GBR Dynamic SedNet model used for catchment load assessment uses paddock-scale models to determine flows into sub-catchments for the 1986–2014 time period. To extend the forcing through to 2017, an empirical approximation of the paddock-scales was used as inputs into the GBR Dynamic SedNet model.

Two GBR Dynamic SedNet scenarios. The first scenario uses present land-use patterns, and is referred to as the Baseline scenario. The same catchment model has been run with catchment vegetation restored to an estimate of pre-1850 cover, but run with the observed rainfall of 2010–present, and with existing water infrastructure such as dams in place, and is referred to as the Pre-Industrial scenario. The loads coming from the Pre-Industrial scenario are referred to as natural loads. The difference between the Baseline and Pre-Industrial loads is referred to as the anthropogenic loads (Brodie et al., 2017). The full details of the Baseline and Pre-Industrial scenarios are given in McCloskey et al. (2021) and Baird et al. (2021).

By running the eReefs coupled hydrodynamic, sediment and biogeochemical model under both Baseline and Pre-Industrial catchment loads, but with identical climatic and ocean forcing, the difference between the coral bleaching in the two scenarios can be used as an estimate of the impact of anthropogenic nutrient and sediment loads on runoff-exposed reefs.

2.3. eReefs coupled hydrodynamic–biogeochemical model

The eReefs model (Fig. 2) simulates the circulation, optics, biogeochemistry and sediment dynamics using the CSIRO Environmental Modelling Suite (EMS, https://github.com/csiro-coasts/EMS). More details on the model grid and hydrodynamic configuration are given in Herzfeld and Gillibrand (2015) and Herzfeld (2015). The sediment (Margvelashvili et al., 2016), optical (Baird et al., 2016) and biogeochemical (Mongin et al., 2016) models are similarly described in detail, with a further 600+ pages documenting model configuration and skill assessment (Herzfeld et al., 2016; Skerratt et al., 2019).

2.3.1. GBR-wide configuration

The eReefs coupled hydrodynamic, optical, sediment and biogeochemical model has been configured at ~1 km resolution for the northeast Australian continental shelf, from 28°40′S to the Papua New Guinea coastline and run from December 1, 2014–present. The model's curvilinear grid has 2389 cells in the alongshore direction, 510 in the offshore direction, and 44 depth levels. The hydrodynamic model is run with a 1.2 s barotropic time step, and the current fields used to calculate mass conserving transport of sediment and biogeochemical constituents (Gillibrand and Herzfeld, 2016). The sediment and biological processes are integrated using a 1 h time step.

The model is forced using atmospheric conditions from the Bureau of Meteorology ACCESS-R and OceanMaps atmospheric and ocean products. Additionally, a 1.21 mg N m^{-2} d^{-1} atmospheric flux into the ocean of ammonium is applied uniformly in time and space across the entire grid, corresponding in regions with an annual rainfall of 1500 mm to a rainwater concentration of 0.3 mg L^{-1} (Packett, 2017). Both the Baseline and Pre-Industrial scenarios used identical atmospheric and ocean boundary conditions. The river flows for the two load scenarios were also the same, but the concentrations of Dissolved Inorganic Nitrogen (DIN), Dissolved Organic Nitrogen (DON), Particulate Nitrogen (PN), Dissolved Inorganic Phosphorus (DIP), Dissolved Organic Phosphorus (DOP), Particulate Inorganic Phosphorus (PIP) and Total Suspended

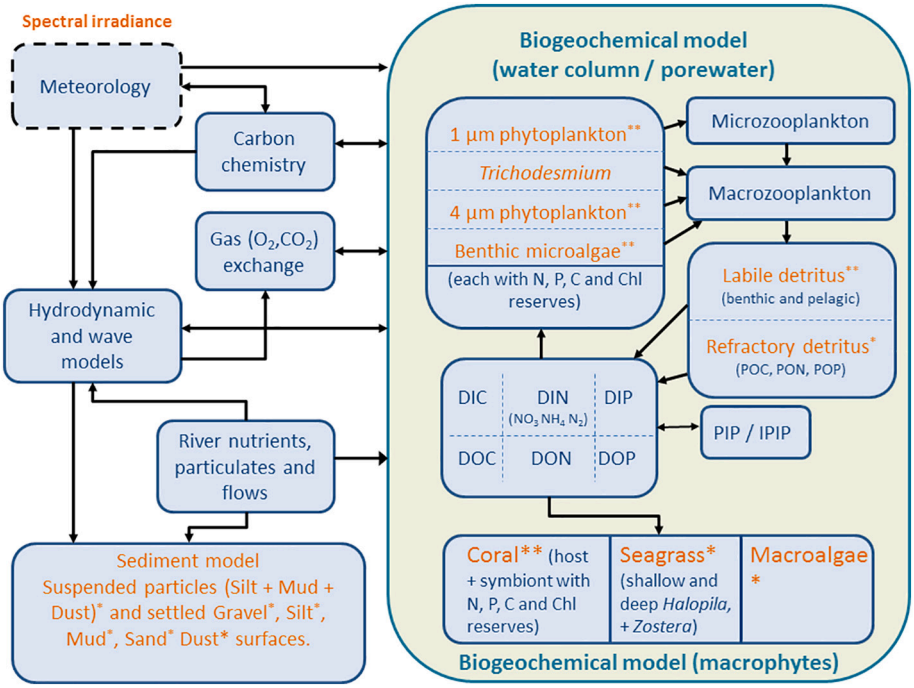

Fig. 2. Schematic showing the eReefs coupled hydrodynamic, sediment, optical, biogeochemical model. Orange labels represent components that either scatter or absorb light, thus influencing seabed light levels.

Sediments (TSS) were adjusted to match the predicted loads of the two scenarios, described in the next two paragraphs.

The model considers inputs of dissolved and particulate constituents from 21 rivers along the Queensland coast (for the location of these rivers boundaries see Skerratt et al. (2019)). The Queensland rivers (north to south) are Normanby, Daintree, Barron, combined Mulgrave and Russell, Johnstone, Tully, Herbert, Haughton, Burdekin, Don, O'Connell, Pioneer, Fitzroy, Burnett, Mary, Calliope, Boyne, Caboolture, Pine, combined Brisbane and Bremer, and combined Logan and Albert. The model also has input from the Fly River in Papua New Guinea. River concentrations of sediment and nutrient for the 4 southern rivers and the Fly were based on mean values from observations over a 10 year period (Furnas, 2003) and multiplied by gauged flows to obtain river loads. The other rivers, the main ones impacting our study region, where based on loads calculated using the GBR Dynamic SedNet model (Waters et al., 2014; Waterhouse et al., 2018).

The model uses a novel river boundary condition (Herzfeld, 2015) that discharges the river freshwater load in a brackish surface plume whose salinity and thickness is calculated to account for upstream flow in a salt-wedge and in-estuary mixing between density layers. The coral distribution in the model is a combination of the eAtlas features map, or, where geographically available, a satellite-derived coral zonation (Roelfsema et al., 2018).

A 5th-order Dormand-Prince ordinary differential equation integrator (Dormand and Prince, 1980) with adaptive step control is used to integrate the local rates of changes due to ecological processes. This requires 7 function evaluations for the first step and 6 for each step thereafter. A relative tolerance of 10^{-4} for each state variable is required for the integration step to be accepted. The mass of carbon, nitrogen, phosphorus and oxygen are checked at each model time step to ensure conservation.

2.3.2. River tracers

The footprint of individual rivers can be calculated using conservative tracers. We use a tracer with a unit concentration (say 100 to represent 100%) in the river flow, resulting in a tracer load proportional to the flow. Thus a location with 50% concentration will be composed of 50% river water, and 50% water either from another river, or oceanic. The tracer is advected and diffused using a conservation flux-form scheme based on hourly-averaged 3D velocity fields (Gillibrand and Herzfeld, 2016). The simulation began tracking plumes on 1 Dec 2014. For more information see Baird et al. (2017).

2.3.3. Reef configurations

Five individual reef sites were chosen to develop 200 m resolution configurations. We chose Jessie Island and High Island because in 2017 they were the sites along the central/northern GBR that were most impacted by river plumes. Further, Havannah Island, Otter Reef and Pandora Reef were chosen to represent a gradient in exposure to plumes, and because they were impacted by different rivers.

The ~200 m configurations were built using the eReefs Project RECOM automatic nesting capability (https://research.csiro.au/ereefs/models/models-about/recom/). The model bathymetry was interpolated from the GBR100 bathymetry (Beaman, 2010) version 4 with improved resolution of reef tops. Atmospheric forcing was the same as the 1 km model above. The initial conditions of each reef for the water column state variables were interpolated from a previous run of the 1 km model: GBR1_H2p0_B1p9_Cfur_Dhnd. Some benthic variables (seagrass and coral distributions) have distributions re-interpolated from the high resolution benthic maps, and assigned values from the nearest neighbour in the 1 km model.

The ~200 m nested model uses boundary conditions provided by a standard eReefs 1 km model simulations that used an earlier version of the coral model that did not include the new photophysiological processes developed in Baird et al. (2018). Thus the 1 km model configuration that generated the boundary conditions for the nested model is slightly different to the nested model itself. Nonetheless, the water column properties that are advected into the nested model, which depend primarily on nutrient/plankton processes in the water column, will be very similar. The boundary condition for all water column tracers was formulated using the advection scheme (Van Leer, 1977) used within the model domain itself. This consistency of boundary and advection schemes ensures diffusion and dispersion errors are minimised.

3. Results

To quantify the impact of natural and anthropogenic loads in the runoff of multiple intermittently-flowing rivers on the physiology of distant zooxanthellae on reefs of the GBR we first characterise the catchment loads, then the extent of the river plumes, and finally the zooxanthellae physiological response at 5 reef sites.

3.1. Catchment loads in early 2017

During the wet season (Dec–May) of 2017, northeast Australia was exposed to low to average rainfall. The rivers of the wet tropics (Herbert, Tully, Mulgrave, Johnstone) had relatively constant flows. The Burdekin, which discharges to the south of our region of interest but whose plume flows northward past the reef sites, had low flow until the passage of Tropical Cyclone Debbie in the last week of March 2017, after the peak of heat stress and bleaching throughout the reef locations. The calculation of loads using GBR Dynamic SedNet is based on the predicted time-varying flow and concentration estimates.

3.1.1. Baseline loads

In the Baseline scenario, from 1 February until mid-March, the Herbert had the largest DIN loads, with the Tully having approximately 40% of the Herbert loads, and very little DIN came from the Burdekin (Figs. 3 & 4, top row). The DIP and sediment loads from the rivers were more similar over the 1 February until mid-March period, with DIP and suspended sediment co-varying. The highest DIP loads were in the Mulgrave. The nutrient loads for the Tully, Herbert, Mulgrave and Johnstone rivers were well above the Redfield ratio (C:N:P = 106:16:1, Redfield et al. (1963)), while the Burdekin loads were approximately Redfield. From mid-March onwards, the Burdekin loads of all constituents increased with the flow associated with Tropical Cyclone Debbie.

3.1.2. Pre-Industrial loads

In the catchment model, the Tully, Johnstone and Mulgrave rivers had approximately half the DIN, DIP and suspended loads in the Pre-Industrial scenario compared to the Baseline scenario, with the N:P ratio staying relatively constant (Figs. 3 & 4, top row). The Herbert Pre-Industrial loads of N decreased more than the P, so the N:P ratio was a little lower. In contrast, as a result of the different land-use patterns, the Burdekin had very similar DIN and DIP loads in the Pre-Industrial scenario compared to the Baseline run, but an order of magnitude less suspended sediment loads.

3.2. Extent of river plumes in early 2017

The mean extent of the river plumes, and time-series of the exposure of each of the 5 reef sites through the simulation period, are given in Figs. 5 & 6. Although the plumes generally travel north from the river mouths, variation due to atmospheric forcing, tides and discharge strength ensure that each of the sites had exposure to multiple plumes. The High and Jessie reefs were chosen due to having the highest total river exposure on the central GBR in 2017, with Jessie having the higher exposure to the Tully, and High to the Johnstone (Fig. 5). The cumulative exposure of all rivers reached a maximum of around 5%. In contrast, Otter, Havannah and Pandora reefs received smaller exposure until late in the simulation when the Burdekin plume reached the Pandora and Havannah sites (Fig. 5).

3.3. Zooxanthellae physiological response at reef site

A snapshot of the surface state variables at Otter Reef exposed to Baseline loads on the 9 April 2017 provides a context for analysis of the modelled zooxanthellae state. Fig. 7 shows the water column variables affecting the coral host and symbiont: temperature, *DIN*, *DIP*, *POM*, as well as the spatially-resolved residence time (age). Other physical variables affecting the corals are climatological seabed temperature (T_{clim}, see Baird et al. (2018) for details of the data used for the climatology), which in combination with present seabed temperature determines the activity of the RuBisCO enzyme (a_{ox}*, which takes a value between 0 inactive and 1 fully active) and the seabed photosynthetically available radiation (*PAR*). The corals are quantified by the biomass of the host, here converted to a percent coverage as seen from above using 100 $(1 - \exp(-\Omega B))$, where B is the biomass, and Ω is the nitrogen-specific polyp area coefficient.

The zooxanthellae is quantified by the nitrogen biomass of the

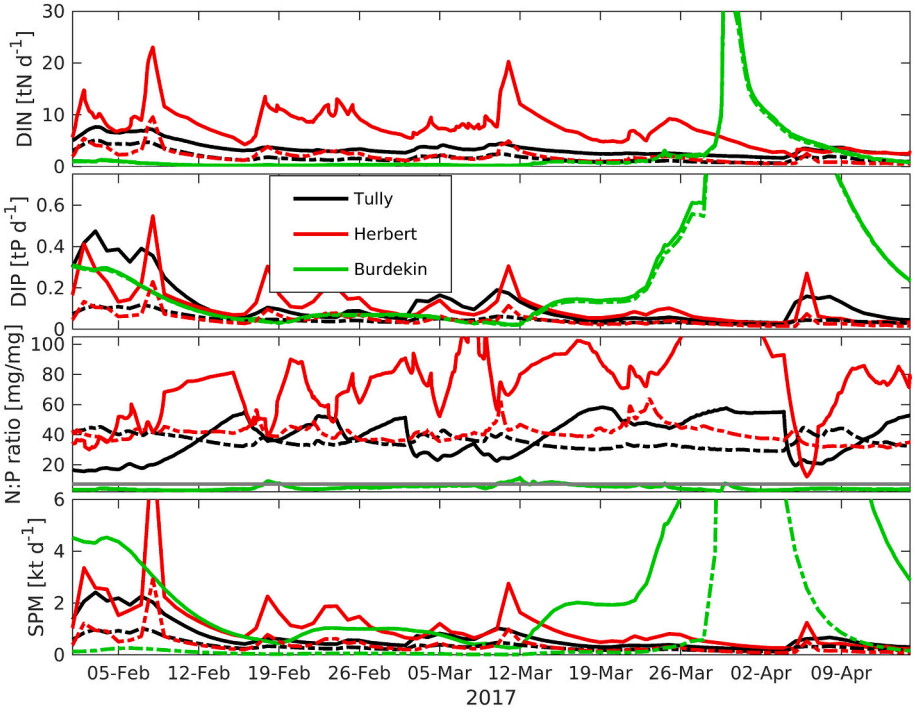

Fig. 3. Catchment Dissolved Inorganic Nitrogen (top), Dissolved Inorganic Phosphorus (2nd top), N:P ratio (3rd top) and Suspended Particulate Matter (bottom) loads from the Baseline (solid lines) and Pre-Industrial (dashed lines) scenarios (Baseline − Pre-Industrial = Anthropogenic loads) from the Tully (black), Herbert (red) and Burdekin (green) rivers, as predicted by GBR Dynamic SedNet. The grey line on the 3rd panel is the Redfield ratio of 16 mol N mol P^{-1}. (For interpretation of the references to colour in this figure legend, the reader is referred to the web version of this article.)

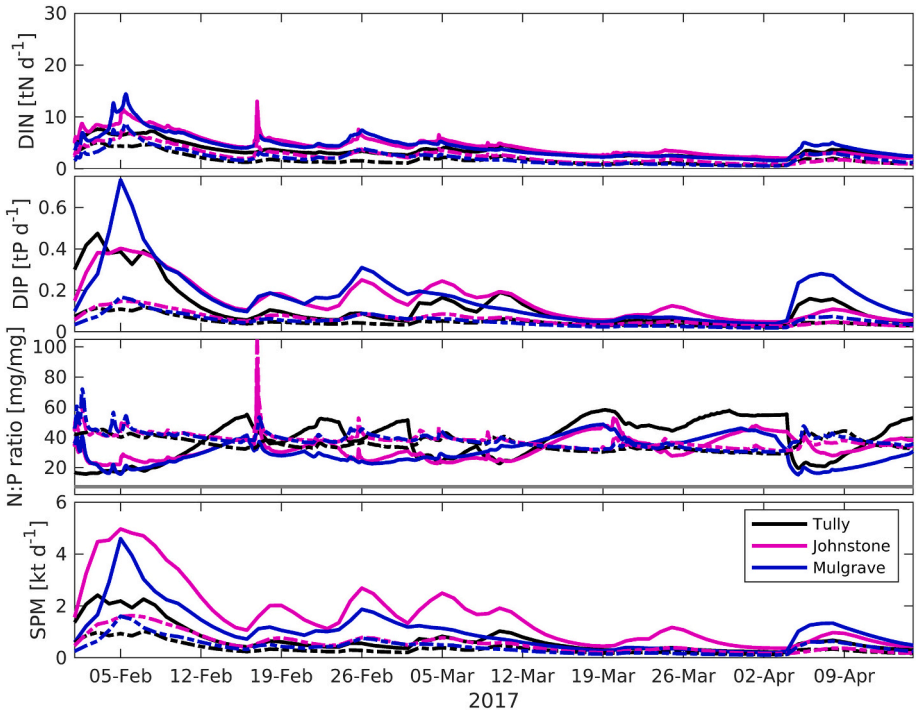

Fig. 4. Catchment Dissolved Inorganic Nitrogen (top), Dissolved Inorganic Phosphorus (2nd top), N:P ratio (3rd top) and suspended sediment (bottom) loads from the Baseline (solid lines) and Pre-Industrial (dashed lines) scenarios (Baseline − Pre-Industrial = Anthropogenic loads) from the Tully (black), Johnstone (pink) and Mulgrave (blue) rivers, as predicted by GBR Dynamic SedNet. The grey line on the 3rd panel is the Redfield ratio of 16 mol N mol P^{-1}. (For interpretation of the references to colour in this figure legend, the reader is referred to the web version of this article.)

cellular structural material (*CS*), and the physiological state by the normalised reserves (a value between zero and 1), of carbon, R_C*, nitrogen, R_N* and phosphorus, R_P*. At Otter Reef for most of the summer of 2017, the concentrations of DIN are low relative to DIP. As a result, at the surface, symbionts are strongly N limited, as demonstrated by $R_N^* \ll R_P^*$, R_C^*. At midday, only the deepest corals show light limitation $R_C^* < 0.5$.

Photoacclimation is quantified by the C:Chl ratio, photoadaptation by the fraction of heat dissipating (X_h) to photoabsorbing (X_p) xanthophyll pigment. The shallowest reefs have the xanthophyll cycle switched to heat dissipating pigments ($X_h > X_p$), but otherwise the pigments are photoabsorbing.

The photosystem state is resolved to oxidised, Q_{ox}*, reduced, Q_{red}*, and inhibited, Q_{in}*. The deepest reef communities on the reef fringe have most of their reaction centres active, while the reaction centre states in the shallower corals in the reef lagoon are 50% inactive.

Finally, a normalised measure of reactive oxygen species, *ROS*, as well as rates of mucus production, inorganic and organic nitrogen uptake, and bleaching are given to understand the model behaviour (Fig. 7). Reactive oxygen build-up is only occurring in the shallowest reef sites. In sites with a seabed depth greater than 20 m, the reaction centres are almost entirely oxidised, and for those less than 5 m they are generally inhibited. At intermediate depths reaction centres are spread across the oxidised, reduced and inhibited states.

For more details to interpret this figure see Baird et al. (2018) which contains a similar figure for Davies Reef on the 22 March 2016. The spatially-resolved state of the other 4 reefs is given in the Supplementary Material.

3.4. Impact of natural and anthropogenic loads on reactive oxygen stress

To look in detail at the impacts of loads on bleaching at the 5 different reefs, we focus on shallow sites on individual reefs (Jessie-Kent, Fig. 8; High, Fig. 9; Havannah, Fig. 10; Otter, Fig. 11; Pandora, Fig. 12) and use time-series of zooxanthellae nutrient status (Panel A), xanthophyll cycle state (Panel B) and reaction centre status (Panel C) to diagnose impacts. Within each figure we show both Pre-Industrial and Baseline to aid in identifying the small differences. Similar time series for deep sites at each of the reefs are shown in the Supplementary Material.

The site with the greatest seabed irradiance was at the mid-shelf Otter reef, due to better water clarity at this offshore location compared to the 4 other near-shore reefs. At Otter Reef, more than 50% of the surface PAR light reached the bottom for the whole simulation period (Fig. 11B). Havannah and Pandora also had high light exposure (generally greater than 50%), while the inshore Jessie (Fig. 8B) and High (Fig. 9B), due to strong water column attenuation, often had less than 20% of the surface light reaching the seabed.

The inshore waters at Jessie (Fig. 8B) and High (Fig. 9B) reef sites had higher thermal anomalies (as shown by longer periods of $a_{Qox}^* = 0$) than the offshore site at Otter Reef. The model, which accumulates reactive oxygen as a function of excess photons reaching the seabed, predicts higher reactive oxygen stress in the midshelf offshore sites than those close to shore.

The contrast between the Jessie, Havannah and Pandora simulations can be discussed in light of the AIMS in-water surveys at each of the reefs in 2017 (Table 2). The in-water surveys showed that all three reefs had high, and approximately equal, thermal stress as measured by NOAA DHWs metric. Similarly, in the model the three reefs showed zero RuBisCO activity, a_{Qox}*, until 6 March 2017 (meaning seabed temperatures >1 °C above the summertime monthly mean), and with similar, slow cooling thereafter. Despite similar thermal stress, the in-water survey suggested more bleaching at Havannah than Pandora or Jessie. In the model, of the three reefs, the physiological state of zooxanthellae at Havannah showed the greatest switching of xanthophyll pigments to the photoprotective (heat dissipating) form, the highest fraction of inhibited reaction centres, and the greatest number of inhibited reaction centres (Fig. 10). Havannah was also the most nutrient depleted of the sites, with normalised reserves of nitrogen of the zooxanthellae, R_N*, being less than 0.1 through the simulations (Fig. 10, red line).

In summary, the observations and model both show greater bleaching stress in the less river-exposed Havannah reef than at Pandora or Jessie. Similarly, the modelled reactive oxygen stress per symbiont was higher at Havannah than at the other two reefs. Jessie showed far less physiological response to the combined thermal and light stress, while Pandora was mid-way between the two. In the model the slightly more

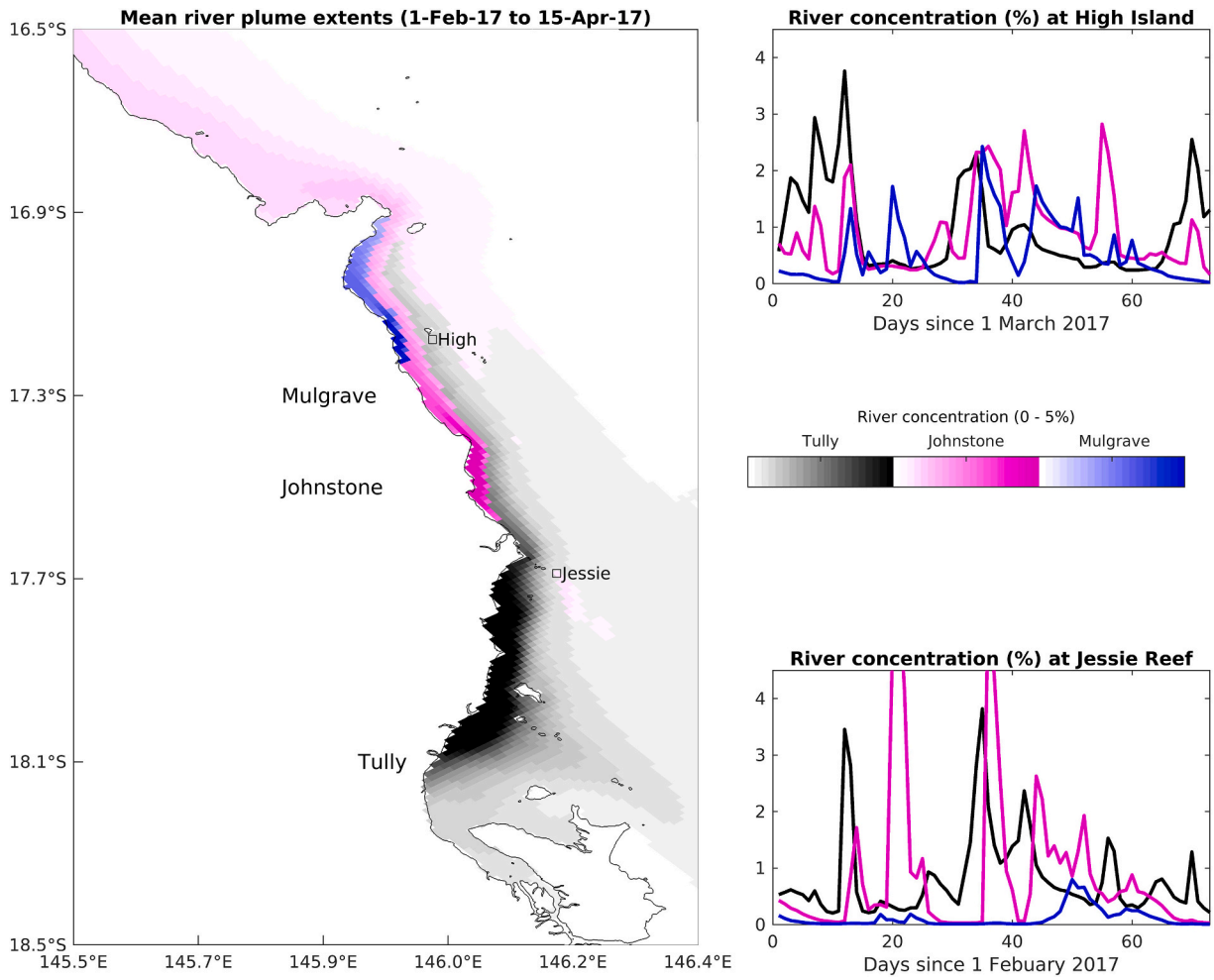

Fig. 5. Temporal-mean spatial extent of the Tully, Mulgrave and Johnstone River plumes in the vicinity of High Island and Jessie Island reefs. Rivers are discharged with a concentration of 100%. At each location the plume colouring only shows the dominant plume over the time period. For view of river plumes across the whole GBR, and the techniques used to calculate the extent, see Baird et al. (2017).

turbid, less nutrient deplete waters above Jessie, and to a lesser extent Pandora, reduced their bleaching stress compared to Havannah. The phenomena of reduced light penetration mitigating coral bleaching has been found in an analysis of 3694 sites from around the globe (Sully and van Woesik, 2020), as well as within local regions (Oxenford and Vallès, 2016).

3.5. Impact of anthropogenic loads on reactive oxygen stress

A comparison of zooxanthellae nutrient status, xanthophyll cycle and reaction centre state with (bottom three Panels) and without (top three Panels) anthropogenic loads at the 5 shallow sites (Jessie-Kent, Fig. 8; High, Fig. 9; Havannah, Fig. 10; Otter, Fig. 11; Pandora, Fig. 12) shows that anthropogenic loads had only a small effect.

The reef site with the greatest change in zooxanthellae physiology as a result of anthropogenic loads was the 4 m deep site on Pandora (Fig. 12). Anthropogenic nitrogen in the Herbert, which impacted on Pandora during February (Fig. 6), resulted in zooxanthellae switching from being N limited ($R_N^* < R_P^*$, Fig. 12A) to P limited. At Pandora, due to the anomalously high temperature (Fig. 12B, $a_{ox}^*=0$), carbon fixation was zero, and carbon reserves became depleted in both load scenarios (Fig. 12A). However when the temperature stress reduced on day 98 (Fig. 12B, $a_{ox}^*>0$), with more nutrient reserves, the growth rate of zooxanthellae increased more in the Baseline scenario than the Pre-Industrial scenario (Fig. 12A, light blue).

The running monthly mean of the seabed PAR at Pandora over the simulation period with Pre-Industrial loads was 11.71 mol photon m^{-2} d^{-1}. Anthropogenic loads slightly reduced the water clarity, reducing seabed light slightly to 11.67 mol photon m^{-2} d^{-1}. This very small change in light intensity resulted in more active xanthophyll switching on days 89–93. With this acclimation, and only a small change in water clarity, the anthropogenic loads had a negligible effect on reactive oxygen stress (Fig. 12C).

The other reef sites did not show a switching of nutrient limitation (Figs. 8A, 9A, 10A, and 11A), and also had only small changes in PAR and reactive oxygen stress.

4. Discussion

The recent mass coral bleaching on the GBR, and globally, has led to a scramble to find means to reduce the decline in reef ecosystems (National Academies of Sciences, Engineering and Medicine, 2019). Managers of coral reef ecosystems have looked for local solutions of which they have control (Anthony et al., 2020; Baird et al., 2020). On the GBR, water quality improvement is the most significant local management strategy for improving reef health (Waterhouse et al., 2017). At the same time, studies have suggested mechanisms through which poor water quality can increase bleaching rates (Wooldridge, 2009). Thus if reducing anthropogenic loads reduces bleaching it would provide a means for local management strategies to simultaneously address two of the greatest threats to the GBR.

This study finds that reducing anthropogenic nutrient and sediment

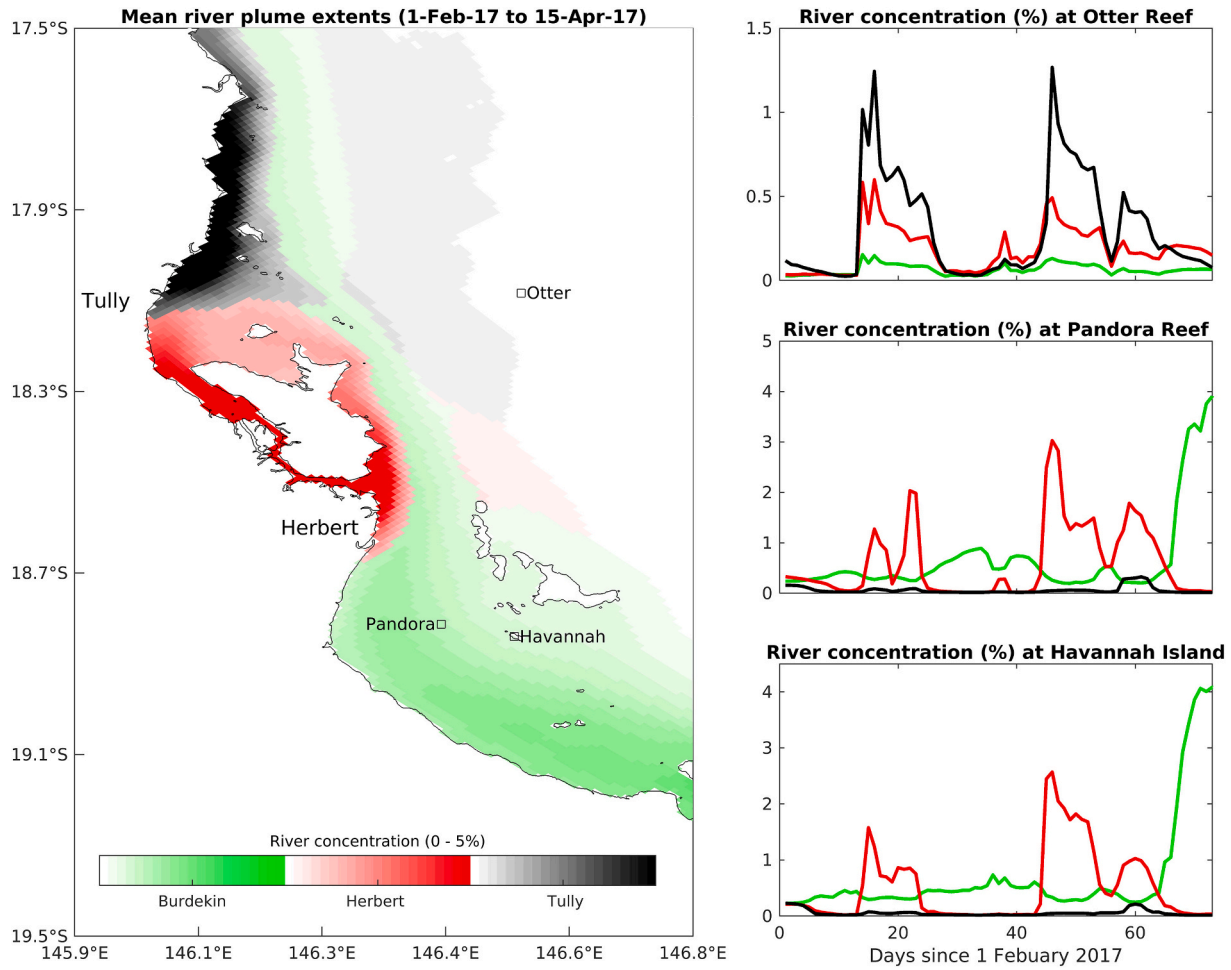

Fig. 6. Temporal-mean spatial extent of the Burdekin (green), Herbert (red) and Tully (black, same as shown in Fig. 4) river plumes in the vicinity of Otter Reef, Havannah Island and Pandora Reef. Rivers are discharged with a concentration of 100%. At each location the plume colouring only shows the dominant plume over the time period. For view of river plumes across the whole GBR, and the techniques used to calculate the extent, see Baird et al. (2017). (For interpretation of the references to colour in this figure legend, the reader is referred to the web version of this article.)

loads during the wet season of 2017 would have had limited influence on the bleaching severity of GBR reefs in 2017. Importantly, the simulations do not consider the effects of loads in earlier wet seasons on coral health leading into 2017, or the impact of loads in recovery of corals after the bleaching.

This discussion first focuses on the uncertainties in the coral model formulation and catchment model forcing, and then provides an explanation of the model's prediction of a negligible effect of anthropogenic loads on bleaching in 2017.

4.1. *Representation of coral bleaching physiology*

The coral model used in the simulations in this paper has been described at length in Baird et al., 2018, where a number of limitations are discussed. Mostly Baird et al. (2018) discussed the uncertainties related to the estimation of model parameters for ROS dynamics. Here we expand the discussion of the limitations to a number of emerging phenomena observed in laboratory studies of coral physiology.

4.1.1. *Nutrient limitation*

In the model, nutrient limitation can lead to lower zooxanthellae growth rates, and, over time, lower cell densities. The simulations considered in this study were from 2017, a relatively low flow year, following on from two very low flow years. Thus nutrient limitation was an important process in the simulations of 2017.

4.1.1.1. *Nitrate versus ammonium uptake.*

In the model at non-limiting concentrations, zooxanthellae preferentially take up ammonium relative to nitrate. If ammonium concentration drops to levels that cellular demand cannot be met due to diffusion limit of uptake, then nitrate uptake provides the remaining nitrogen. However, the model does not impose any energetic cost to nutrient (ammonium, nitrate or phosphorus) uptake. Rather the model applies a generic basal respiration rate representing all the costs of metabolic processing (Baird et al., 2018, Eq. A.7). As a result, the model cannot resolve the difference in energetic costs between nitrate and ammonium uptake (Morris et al., 2019) which is likely to lead to the model underestimating carbon limitation during low ammonium/high nitrate conditions. In the context of bleaching, if carbon fixation is inhibited by high temperatures, the model will underestimate the time it takes for carbon reserves to be depleted under low ammonium concentrations.

4.1.1.2. *Nitrogen and phosphorus recycling.*

A key reason for the ability of corals to survive in low nutrient waters is the recycling of nutrients (or translocation between host and symbiont). Translocation is represented in the model with identical pathways for N and P. However due to the different roles N and P play in biological molecules (DNA, ATP, photosynthetic phospholipids), it may be that N is more efficiently recycled than P. Furthermore, high N:P ratios have been especially associated with increasing coral bleaching susceptibility (Wiedenmann et al., 2013; Morris et al., 2019).

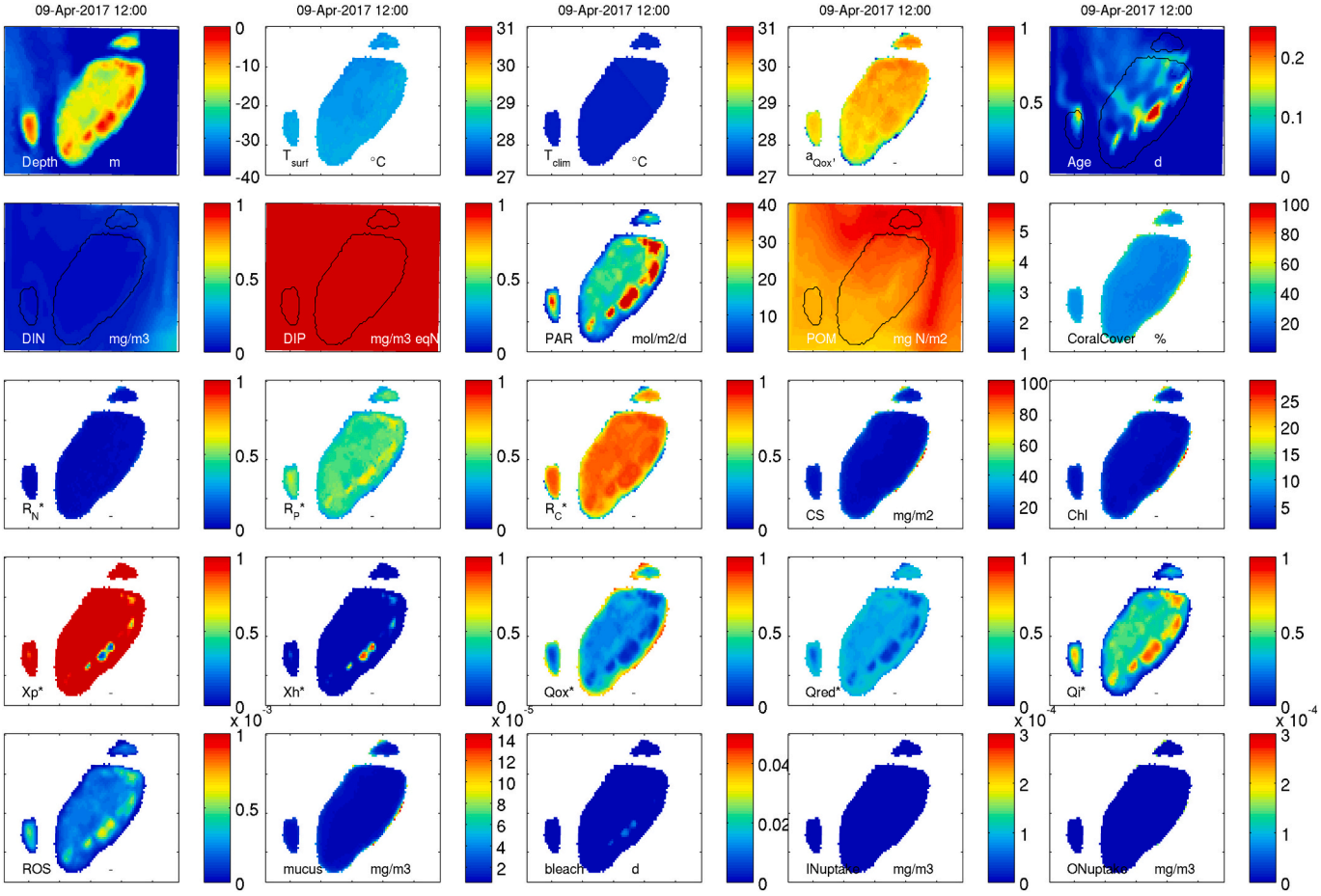

Fig. 7. Coral-related state variables at midday on 9 April 2017 in the ~200 m nested model at Otter Reef exposed to Baseline catchment loads. Variables that are shown only on the reef are seabed values (i.e. PAR is downwelling light just above the coral surface), while DIN, Age, DIP, and POM are near surface fields with off reef values shown. The * refers to a normalised value, such that reserves of C, N, and P are values between 0 (deplete) and 1 (replete), while the sum of normalised xanthophyll pigments ($X_h^* + X_p^*$) and normalised reaction centres ($Q_{ox}^* + Q_{red}^* + Q_{in}^*$) is 1. Abbreviations given in Table 1.

4.1.2. Relationship between reactive oxygen stress and zooxanthella expulsion

In this paper we have restricted our results to the build-up in ROS within a zooxanthella cell, rather than present a coral bleaching rate. To extend the model analysis to calculate the rate of bleaching is problematic because the relationship between ROS and the rate of zooxanthellae expulsion is complex. In this paper and Baird et al. (2018) we used laboratory experiments of Suggett et al. (2008) to estimate the concentration of ROS at which expulsion is initiated. We then composed a linear relationship between expulsion rate and the concentration of ROS above that threshold, fitting the results from the 1 km resolution model to spatial distribution of bleaching in 2016 (Hughes et al., 2018b). While the approach of fitting to observations ensures a reasonable prediction of the data set, errors are to be expected when applying this parameterisation at a different time or location.

Perhaps an even more significant limitation to our model representation of the bleaching rate is that it does not explicitly consider the role of the host. Host control of bleaching can include both preventative measures such as reducing reactive oxygen concentrations as well as actively facilitating cell expulsion (Baird et al., 2009) and controlling the access of the symbionts to dissolved nutrients (Cui et al., 2018). Given the empirical nature of the expulsion term we used, the model will implicitly include some of these host-driven processes. However, since the expulsion is explicitly dependent on ROS per cell, it cannot even implicitly represent host-driven processes that are dependent on the ROS per polyp.

A number of papers have considered the possibility of host-driven expulsion due to heat stress destabilizing symbiotic nutrient cycling between the host and the symbiont. (Wooldridge, 2020; Rädecker et al., 2021). Thus the role of the host in responding to oxidative stress is affected by supply of inorganic nutrients even though the host only uses the organic carbon produced by the symbiont. In the model presented in this paper, nutrient supply and temperature interact to determine carbon fixation. Thus some of the nutrient - bleaching relationships of Rädecker et al. (2021) and others related to supply of organic carbon could be explained by processes already represented in our model. Ultimately, however, the model needs to be extended to explicitly consider host responses to organic carbon supply, temperature and oxidative stress.

An additional impact of nutrient loads is an increasing density of zooxanthellae, which leads, for a given zooxanthella physiological state, to a greater build-up of ROS in the coral polyp. In the case of the analysis of anthropogenic loads of 2017 in this paper, when nutrient concentrations were low, and cell densities were only allowed to evolve from 1 Dec 2016, the impact of cell densities on coral bleaching are likely to be small. However, this will not necessarily be true during years with greater catchment loads prior to the bleaching period.

4.2. The catchment model calculation of anthropogenic loads

In this study we have determined the combined impact of anthropogenic sediment and nutrient loads by comparing the different behaviour of the bleaching model for two catchment model runs: Baseline, an estimate of today's catchment loads, and Pre-Industrial, an

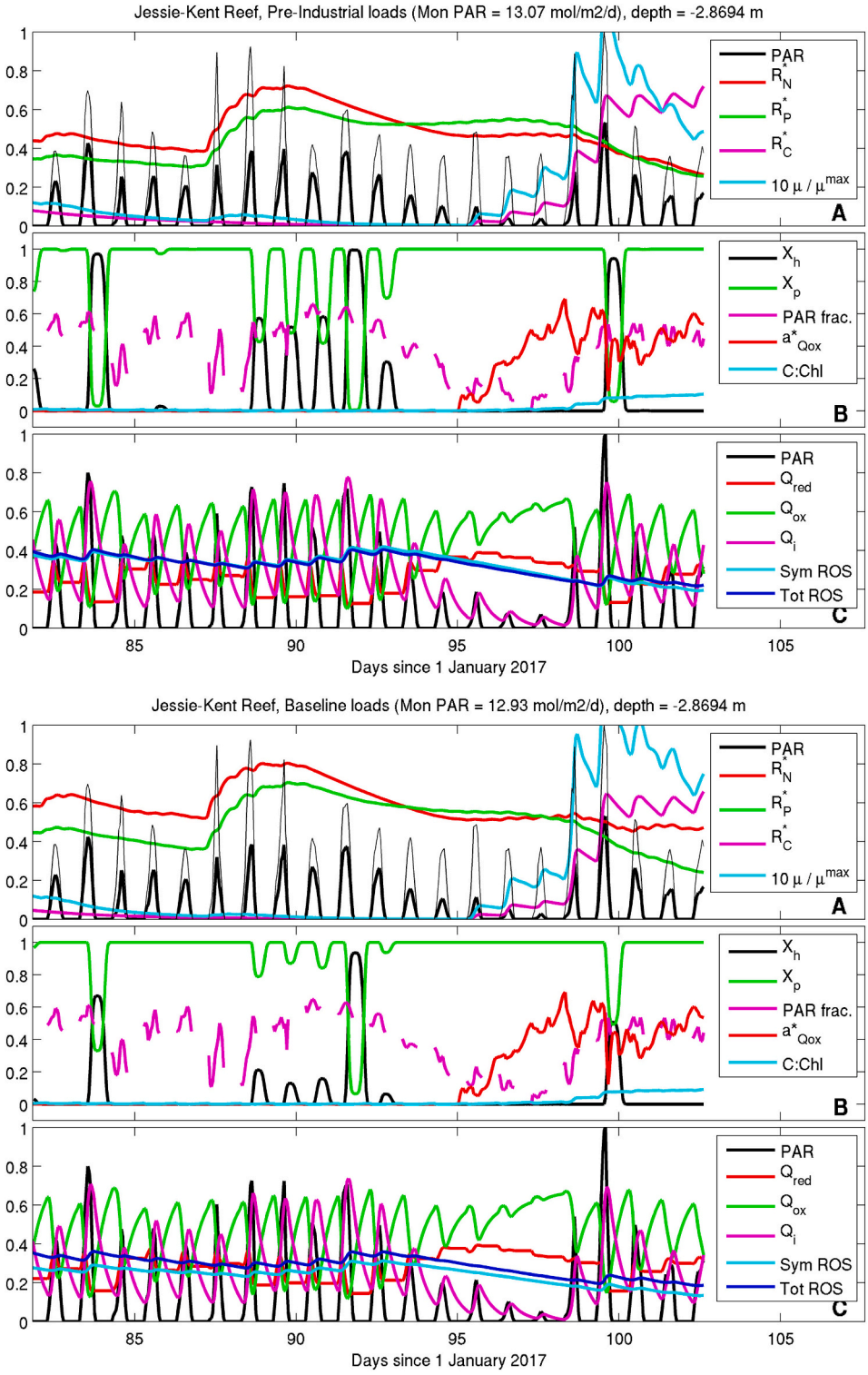

Fig. 8. Model behaviour near Jessie-Kent Island at a shallow site with an approximation of Pre-industrial catchment loads (top 3 rows) and with anthropogenic loads added (bottom three rows) site. Panels A show the light at sea surface (line black line) and at the coral surface (PAR, mol photon m^{-2} d^{-1}, scaled on the *y*-axis to the monthly running mean PAR over the period given in the title), and the normalised reserves of nitrogen, phosphorus and carbon. The normalised growth rate is also shown. Panel B shows the state of the xanthophyll cycle as the fraction of heat absorbing (X_h) and heat dissipating (X_p) pigments, the RuBisCO activity (a_{Qox}*, varying between inactive at 0 and fully active at 1), the carbon to chlorophyll-*a* ratio (scaled on the *y*-axis so the minimum C:Chl ratio of 20 g/g is 0, and 1 is 180 g/g), and the fractional reduction in PAR from the surface. Panels C show the state of the reaction centres, and the concentration of reactive oxygen per cell in the symbiont above a threshold value that initiates zooxanthellae expulsion (mg O $cell^{-1}$), as well as the total reactive oxygen per coral host. Abbreviations given in Table 1.

estimate of loads with pre-1850 vegetation cover. While uncertainties exist in both these estimates, the difference between the two estimates can be calculated exactly.

The GBR-wide load scenarios that the fine resolution models were nested into started on 1 December 2014. Thus, the boundary condition of the two scenarios of the nested models (which started on 1 December 2016) resulted from the cumulative impacts of three years of different loads. Of those years, 2015 and 2016 were particularly dry years. Dry years deliver low loads and small differences between the Baseline and Pre-Industrial scenarios. So there will not be a large local legacy effect of the different catchment scenarios. The initial condition of both the nested models themselves was constructed from the GBR1 configuration Baseline scenario.

From Fig. 3 we can see on 1 February 2017 that the estimated suspended sediment load in the Baseline scenario is approximately 4 kT day^{-1} greater than the Pre-Industrial scenario. Thus the different bleaching response of the two scenarios can be thought of the effect of removing 4 kT day^{-1} on that day (and corresponding reductions

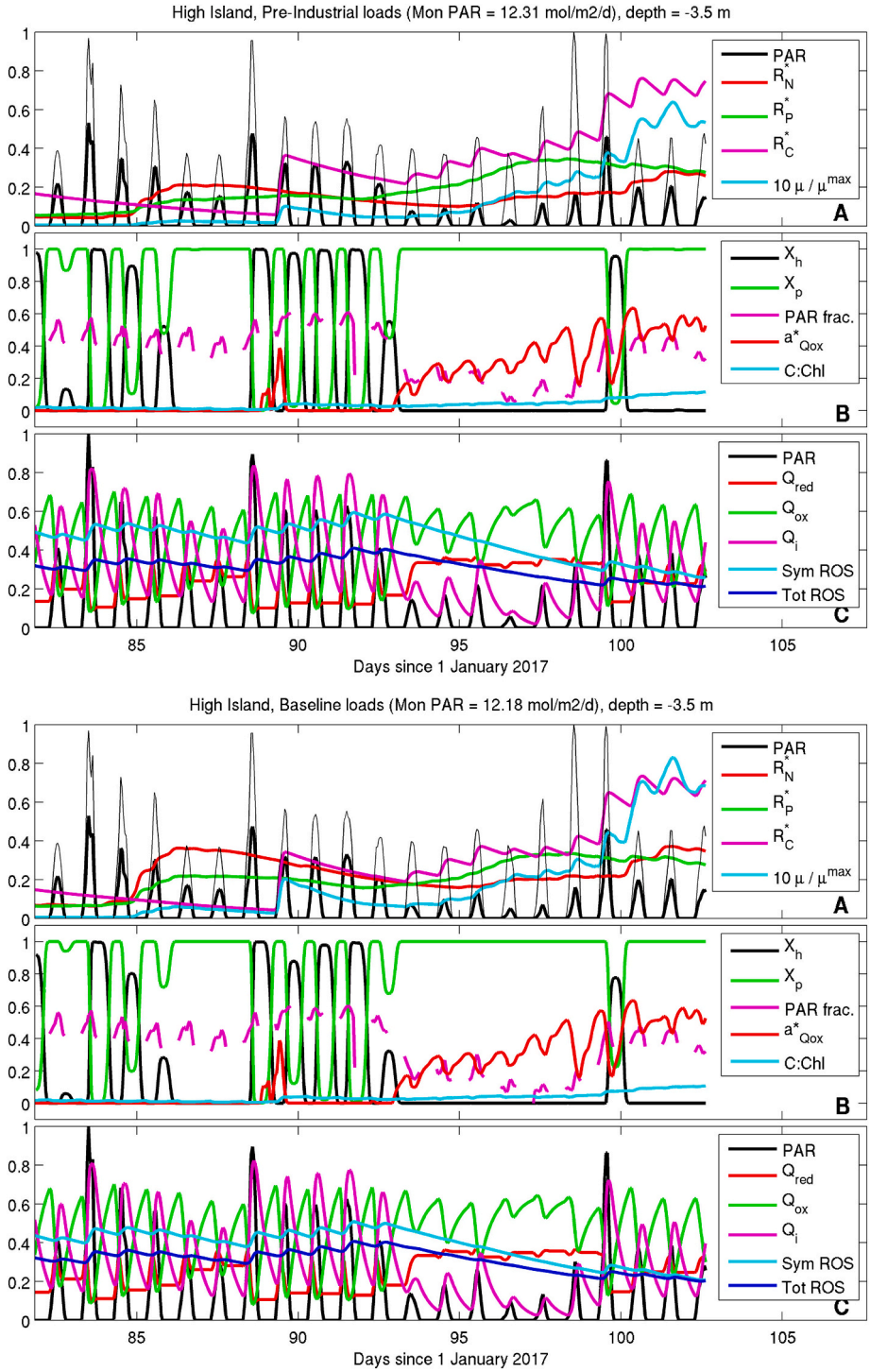

Fig. 9. Model behaviour at High Island at a shallow site. See Fig. 8 for full caption.

following Fig. 3 on the subsequent days). Whether or not 4 kT day^{-1} is a good estimate of the anthropogenic loads on 1 December 2016 is a somewhat academic calculation, as vegetation cover is unlikely to return to the pre-1850s state. Nonetheless, the 4 kT day^{-1}, and its time-varying values, represents a quantity against which real management strategies can be evaluated (Brodie et al., 2017).

4.3. Impact of anthropogenic loads in 2017

The most severe threat to tropical coral reef ecosystems is ocean warming and widespread coral mortality due to increasingly frequent and severe coral bleaching events (Hughes et al., 2018a). The largest local investment in environmental protections for the GBR is the $2 billion Reef 2050 plan, which up until 2019 has focused on catchment repair to improve water quality (Brodie et al., 2017).

The simulations presented in this paper show a small, even negligible, effect of river-derived anthropogenic loads on reactive oxygen stress build-up in five sites chosen for their relatively high potential exposure to rivers. That is, the simulations predict that had all anthropogenic loads been removed from GBR rivers from 1 Dec 2016 to 1 April 2017, there would have been no change in the zooxanthellae physiological response or bleaching severity under the heating observed up to

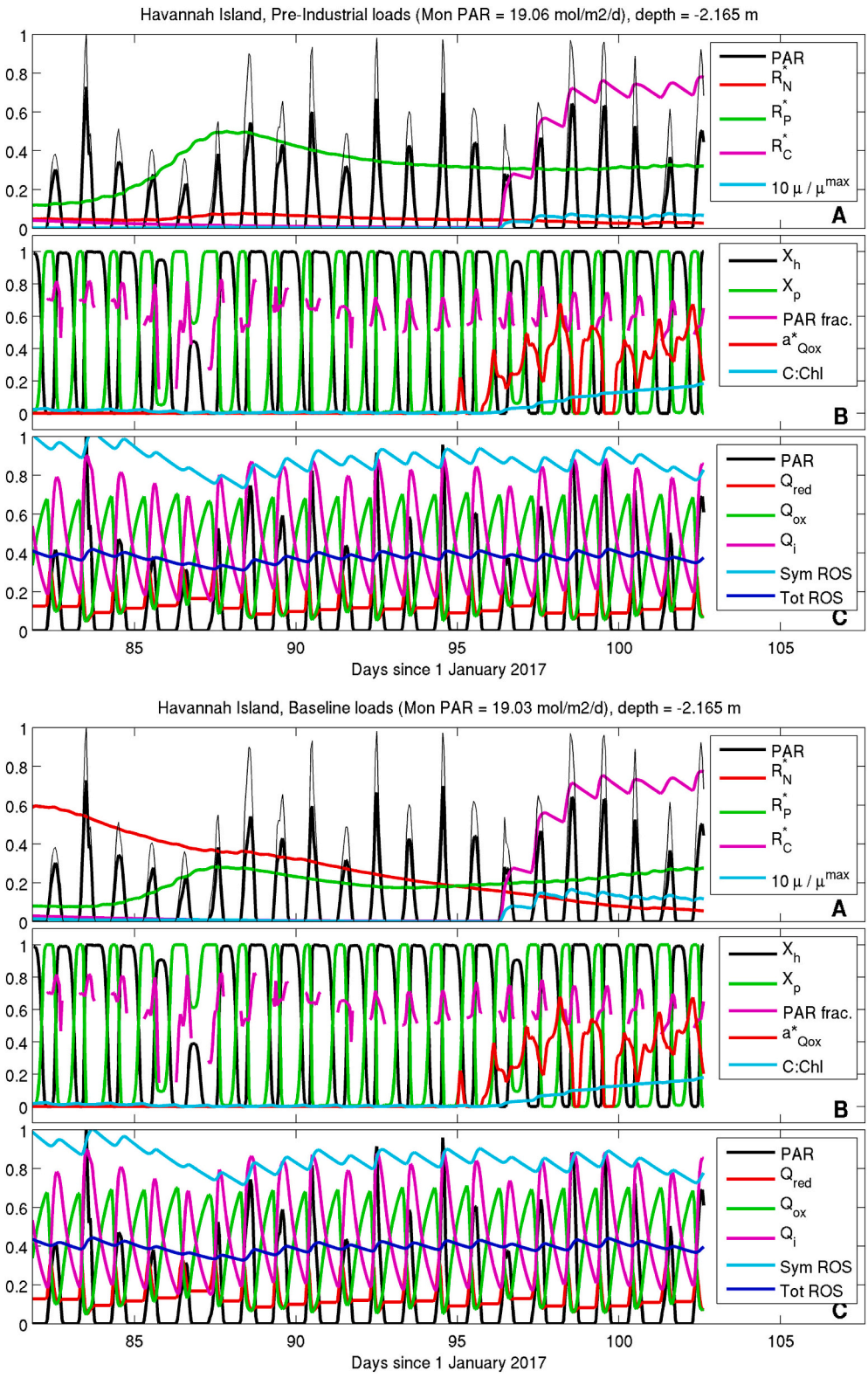

Fig. 10. Model behaviour at Havannah Island at a shallow site. See Fig. 8.

mid-March 2017.

Prior to the 2017 GBR bleaching event, Queensland was in severe drought with annual river discharge into the study region from 2013 to 2017 2.3 fold below median levels. It will be important to undertake a similar study in a bleaching year with above average rainfall, such as 2020. However, it is worth noting that years with anomalously high ocean temperatures are more likely to occur during years with weak monsoon activity, less cloud cover, rainfall and therefore less river discharge. Thus, for the purposes of justifying catchment load reductions to reduce coral bleaching, the most relevant years are 2016 or 2017. This study shows that in 2017 further catchment repair would not have changed the transport of anthropogenic loads into the GBR to a level that

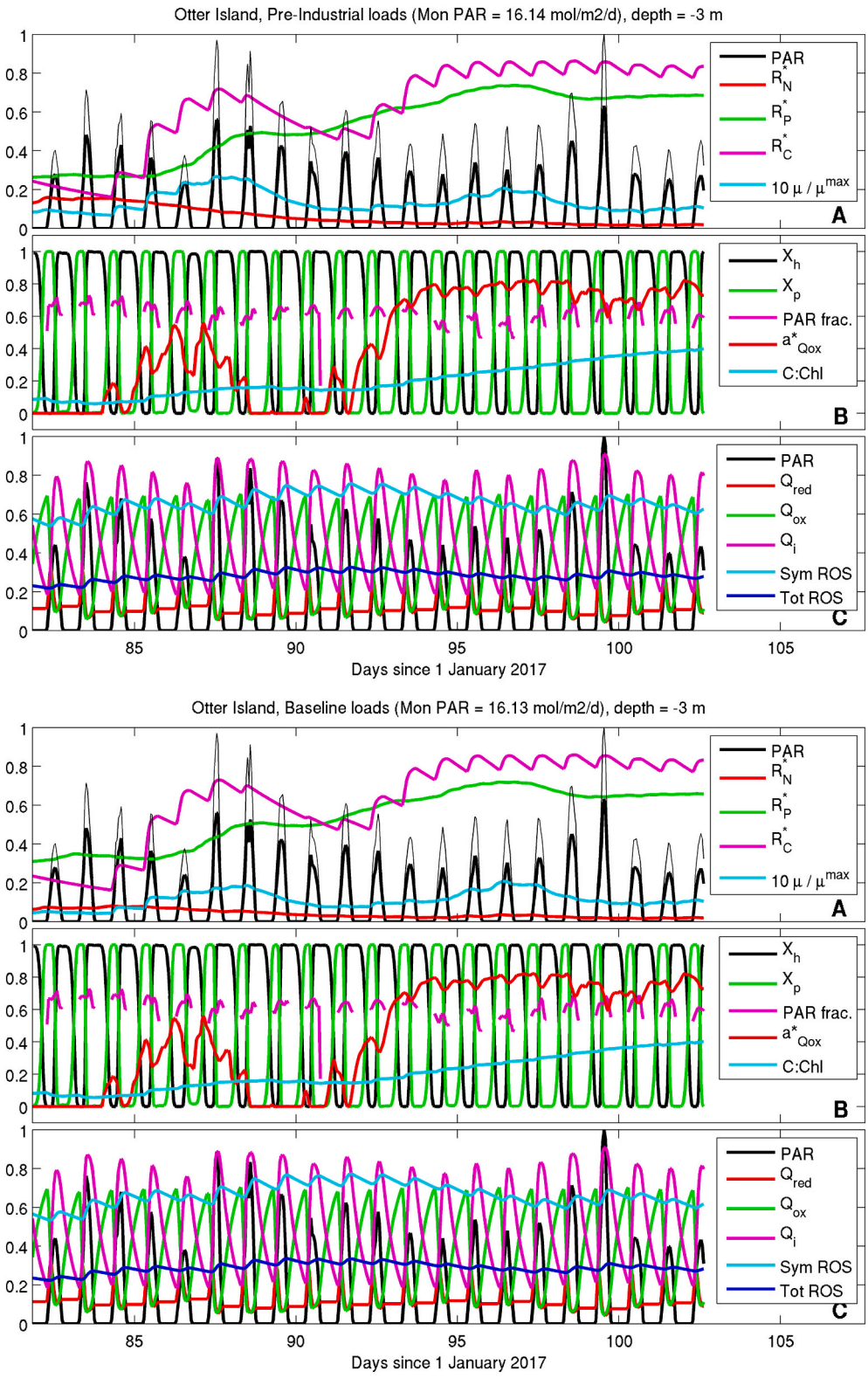

Fig. 11. Model behaviour at Otter Island at shallow site. See Fig. 8.

would have influenced the levels of thermal oxidative stress leading to coral bleaching. The major reasons for this are:

(1) In 2017 catchment flows were low, resulting in relatively small differences between natural and anthropogenic loads (Figs. 3 & 4).

(2) The low flows led to small plume extents, which are constrained to propagate north in a thin inshore region by the rotation of the Earth; thus the reefs considered, some of the most exposed in the GBR, were generally exposed to waters of less than 4% freshwater (Figs. 5 & 6), and therefore highly diluted terrestrial inputs.

(3) Reefs are generally located at least a few tens of kilometres downstream from river plume mouths due to the toxic effect of freshwater exposure on corals. At this distance from the river mouth sediment

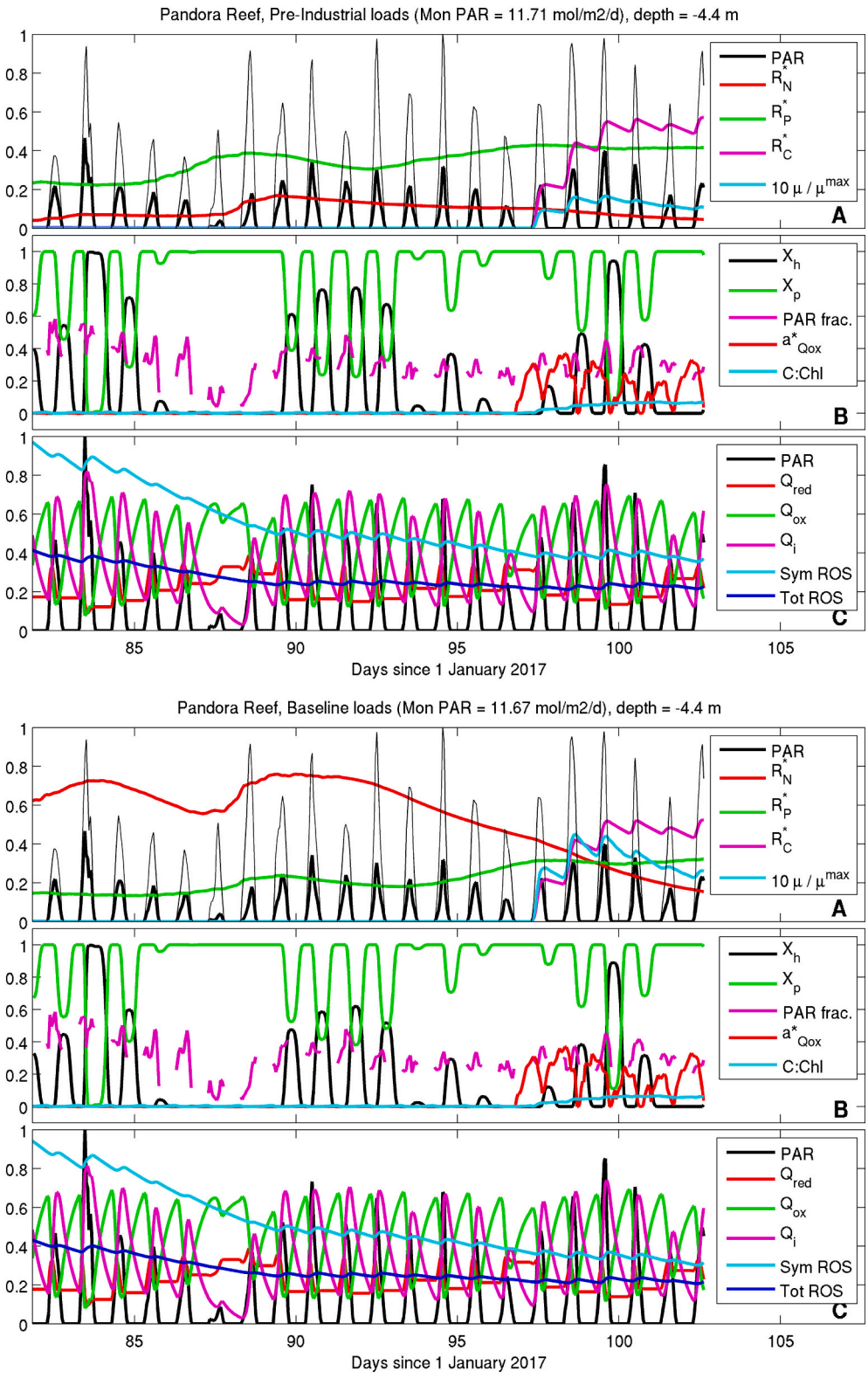

Fig. 12. Model behaviour at Pandora Island at shallow site. See Fig. 8.

plumes have generally sunk out of the water column (Margvelashvili et al., 2016). Although these deposits may be subsequently resuspended, the resuspension is composed of a small fraction of recent anthropogenic loads and a much greater fraction of loads deposited over many years. As a result of similar suspended sediment loads in 2017, under natural loads there is very little difference in bottom light intensity due to anthropogenic loads.

(4) Other than changes in the seabed light intensity, the main mechanism for runoff to affect zooxanthellae physiology is through changing water column nutrient concentrations. Dissolved tracers propagate further in the plume than the sediments. However during low flow years, when the coastal waters are deplete in nutrients, microalgae,

Table 2
Data from the AIMS in-water surveys at shallow sites in 2017. DHW — NOAA degree heating weeks metric on the day of survey; Bleached — percent of all corals >5 cm in size scored as bleached.

Site	Depth [m]	DHW [°C]	Bleach [%]
Jessie (Nth Banard MMP1)	3	7.3	43
Pandora (NW Flat)	3	6.7	34
Havannah (Island Flat)	5	6.0	52

seagrass and seaweeds all compete strongly for nutrients, resulting in very low nutrient concentrations at the coral seabed, even under anthropogenic loads (Skerratt et al., 2019).

(5) What excess nutrients do make it to the reefs are then potentially taken up by the coral community (Atkinson, 1992). The absorbed nutrients can then be used by the zooxanthellae for growth, and in the process consuming fixed carbon reserves. With lower fixed carbon reserves, excess photons can be consumed by carbon fixation required to replenish the carbon reserves. But nitrogen and phosphorus reserves can only impact on the build-up of reactive oxygen by increasing the rate of carbon fixation, which only occurs if the RuBisCO enzyme is active ($a_{ox}^{*}>0$). Thus the inactivation of the RuBisCO enzyme acts to prevent runoff-derived nutrients, either natural or anthropogenic, having an impact on the build-up of ROS.

(6) The zooxanthellae use photoadaptation (changing pigment synthesis rates to alter pigment content) and photoacclimation (xanthophyll switching between photosynthetic and heat dissipating forms) to suppress the impact of excess photons. These processes, at least in the model, are independent of nutrient status and thus runoff-derived loads.

(7) In the model, reactive oxygen stress is quantified by cell, and per host. The flux of photons to each cell, and to the host, is reduced if the zooxanthellae cell density, or host tissue biomass respectively, becomes large enough to self-shade. While the light and nutrient environment potentially varies cell and host density, this is constrained by the anatomy of the coral host that only allow only 2 layers of symbiont cells.

Thus the model simulations suggest nutrient and sediment loads from human activities did not significantly change the severity of coral bleaching on the GBR in 2017. This is most likely due to the significant drought phase of the climate cycle, low terrestrial input and transport of sediment and nutrients following well below median rainfall and river-flow throughout the study region from 2013 to 2017. A similar conclusion was reached by Hughes et al. (2018b), based on field observations of the 2016 bleaching event and using a correlation of coral bleaching severity and seawater chlorophyll-*a* concentrations as a proxy for nutrient enrichment.

While reducing anthropogenic loads provides little prospect of reducing temperature-mediated, light-driven build-up of reactive oxygen stress causing coral bleaching at a particular site, the combination of natural and anthropogenic loads, and the gradient in river exposure across the shelf, results in differing reactive oxygen stress across sites. Quantification of the gradient in reactive oxygen stress, in combination with other stress such as acidification exposure (Mongin et al., 2016), will provide managers with information for future reef planning (Albright et al., 2016).

5. Conclusion

Using a coupled catchment — hydrodynamic–biogeochemical model, this study has distinguished between natural and anthropogenic catchment loads from rivers on the northeast Australian continent, and mechanistically linked the catchment loads and thermal stress to levels of reactive oxygen stress in zooxanthellae at river-exposed reefs of the GBR. The simulations revealed that in 2017, a below average rainfall year, river exposure on the GBR was relatively small. We found for the loads delivered between 1 Dec 2016 and 30 Apr 2017, there was a small difference in ROS stress between inshore and midshelf sites, but virtually no difference when sites exposed to both anthropogenic loads and natural loads are compared to natural loads alone. This negligible influence of anthropogenic loads was due to the relatively small plumes of 2017. It remains to be seen if, in the future, years with strong river discharge, if combined with anomalously high ocean temperatures and high solar radiation, will result in significant impacts of anthropogenic catchment loads on coral bleaching.

The simulations do not capture the impact of loads delivered from previous wet seasons on coral health (Rocker et al., 2019), or the impact of loads delivered in future seasons on recovery from bleaching. In some years, such as 2011, anthropogenic loads can have significant multi-year impacts on the GBR ecosystems that remain a threat to its health (Fabricius et al., 2016; Brodie et al., 2017).

Further work on multi-year impacts of catchment load inputs and resuspension transport dynamics combined with other pressures such as ocean acidification may be important for understanding the links between catchment repair, nutrient and sediment inputs and coral bleaching and recovery. Nonetheless, the negligible impact of anthropogenic loads on coral bleaching in the process-based simulations of 2017 is consistent with the present understanding that coral bleaching on the GBR is driven primarily by ocean temperature anomalies and seabed light levels and also aligns with analysis of 2016 aerial surveys that suggest no relationship between marine water quality and bleaching.

Declaration of competing interest

The authors declare that they have no known competing financial interests or personal relationships that could have appeared to influence the work reported in this paper.

Acknowledgements

The coral bleaching model presented here was developed with funding from CSIRO and the National Environmental Science Program (NESP) Tropical Water Quality Hub (Project No. 3.3.1). The model simulations were developed as part of the eReefs Project, a public-private collaboration between Australia's leading operational and scientific research agencies, government, and corporate Australia. Funding for in water bleaching surveys was provided by the Australian Institute of Marine Science and the NESP TWQ Hub (Project No. 3.3.1). The authors wish to thank the many scientists involved in the eReefs Project, in particular Mike Herzfeld, John Andrewatha, Nugzar Margvelashvili, Karen Wild-Allen, Barbara Robson, Andy Steven and Cedric Robillot. Observations used in the eReefs Project include those from the Integrated Marine Observing System (IMOS) and the Marine Monitoring Program (MMP). We thank Rob Ellis and David Waters for the catchment modelling as part of the Queensland and Australian Government's Paddock to Reef program that is funded by the Queensland Department of Natural Resources and Mines 'Queensland Regional Natural Resource Management Investment Program 2013–2018' with support from the Department of Science, Information Technology, Innovation and the Arts (DSITIA). Thank you to Christopher Doropoulos ideas for improving the manuscript. LM was supported by an AIMS@JCU PhD scholarship and a NESP Tropical Water Quality Hub grant.

Appendix A. Supplementary data

Supplementary data to this article can be found online at https://doi.org/10.1016/j.marpolbul.2021.112409.

References

Albright, R., Alongi, D.M., Anthony, K., Baird, M., Beeden, R., Byrne, M., Collier, C., Dove, S., Fabricius, K., Hoegh-Guldberg, O., Kelly, R., Lough, J., Mongin, M., Munday, P., Pears, R., Russell, B., Tilbrook, B., Abal, E., 2016. Ocean acidification: linking science to management solutions using the Great Barrier Reef as a case study. J. Environ. Manage. 182, 641–650.

Anthony, K., Helmstedt, K.J., Bay, L.K., Fidelman, P., Hussey, K.E., Lundgren, P., Mead, D., McLeod, I.M., Mumby, P.J., Newlands, M., Schaffelke, B., Wilson, K.A., Hardisty, P.E., 2020. Interventions to help coral reefs under global change — a complex decision challenge. PLoS One 15, e0236399.

Atkinson, M.J., 1992. Productivity of Eniwetak atoll reef predicted from mass-transfer relationships. Cont. Shelf Res. 12, 799–807.

Bainbridge, Z., Lewis, S., Bartley, R., Fabricius, K., Collier, C., Waterhouse, J., Garzon-Garcia, A., Robson, B., Burton, J., Wenger, A., Brodie, J., 2018. Fine sediment and particulate organic matter: a review and case study on ridge-to-reef transport, transformations, fates, and impacts on marine ecosystems. Mar. Pollut. Bull. 135, 1205–1220.

Baird, A.H., Bhagooli, R., Ralph, P.J., Takahashi, S., 2009. Coral bleaching: the role of the host. Trends Ecol. Evol. 24, 16–20.

Baird, M.E., Ralph, P.J., Rizwi, F., Wild-Allen, K.A., Steven, A.D.L., 2013. A dynamic model of the cellular carbon to chlorophyll ratio applied to a batch culture and a continental shelf ecosystem. Limnol. Oceanogr. 58, 1215–1226.

Baird, M.E., Cherukuru, N., Jones, E., Margvelashvili, N., Mongin, M., Oubelkheir, K., Ralph, P.J., Rizwi, F., Robson, B.J., Schroeder, T., Skerratt, J., Steven, A.D.L., Wild-Allen, K.A., 2016. Remote-sensing reflectance and true colour produced by a coupled hydrodynamic, optical, sediment, biogeochemical model of the Great Barrier Reef, Australia: comparison with satellite data. Environ. Model. Softw. 78, 79–96.

Baird, M.E., Andrewartha, J., Herzfeld, M., Jones, E., Margvelashvili, N., Mongin, M., Rizwi, F., Skerratt, J., Soja-Woźniak, M., Wild-Allen, K., Schroeder, T., Robson, B., da Silva, E., Devlin, M., 2017. River plumes of the Great Barrier Reef: freshwater, sediment and optical footprints quantified by the eReefs modelling system. In: Syme, G., Hatton MacDonald, D., Fulton, B., Piantadosi, J. (Eds.), MODSIM2017, 22nd International Congress on Modelling and Simulation. Modelling and Simulation Society of Australia and New Zealand, pp. 1892–1898. https://www.mssanz.org.au/modsim2017/L22/baird.pdf.

Baird, M.E., Mongin, M., Rizwi, F., Bay, L.K., Cantin, N.E., Soja-Woźniak, M., Skerratt, J., 2018. A mechanistic model of coral bleaching due to temperature-mediated light-driven reactive oxygen build-up in zooxanthellae. Ecol. Model. 386, 20–37.

Baird, M.E., Green, R., Lowe, R., Mongin, M., Bougeot, E., 2020. Optimising cool-water injections to reduce thermal stress on coral reefs of the Great Barrier Reef. PLoS One 15 (10), e0239978.

Baird, M.E., Mongin, M., Skerratt, J., Margvelashvili, N., Tickell, S., Steven, A.D.L., Robillot, C., Ellis, R., Waters, D., Kaniewska, P., Brodie, J., 2021. Impact of catchment-derived nutrients and sediments on marine water quality on the Great Barrier Reef: an application of the eReefs marine modelling system. Mar. Pollut. Bull. 167, 112297.

Beaman, R.J., 2010. Project 3DGBR: a high-resolution depth model for the Great Barrier Reef and Coral Sea, pp. 13 plus Appendix 1. In: Tech. Rep., Marine and Tropical Sciences Research Facility (MTSRF) Project 2.5i.1a Final Report. MTSRF, Cairns, Australia.

Brodie, J., Waterhouse, J., 2012. A critical review of environmental management of the 'not so Great' Barrier Reef. Est. Coast. Shelf Sci. 104–105, 1–22.

Brodie, J., Baird, M., Mongin, M., Skerratt, J., Robillot, C., Waterhouse, J., 2017. Pollutant target setting for the Great Barrier Reef: using the eReefs framework. In: Syme, G., Hatton MacDonald, D., Fulton, B., Piantadosi, J. (Eds.), MODSIM2017, 22nd International Congress on Modelling and Simulation. Modelling and Simulation Society of Australia and New Zealand, pp. 1913–1919. December 2017.

Clementson, L.A., Wojtasiewicz, B., 2019a. Dataset on the absorption characteristics of extracted phytoplankton pigments. Data Brief. https://doi.org/10.1016/j.dib.2019.103875.

Clementson, L.A., Wojtasiewicz, B., 2019b. Dataset on the in vivo absorption characteristics and pigment composition of various phytoplankton species. Data Brief 25, 104020.

Condie, S.A., Plagányi, E., Morello, E.B., Hock, K., Beeden, R., 2018. Great Barrier Reef recovery through multiple interventions. Conserv. Biol. 32, 1356–1367.

Cui, G., Liew, Y.J., Li, Y., Kharbatia, N., Zahran, N.I., Emwas, A.-H., Eguiluz, V.M., Aranda, M., 2018. Meta-analysis reveals host-dependent nitrogen recycling as a mechanism of symbiont control in Aiptasia. bioRxiv. URL. https://www.biorxiv.org/content/early/2018/02/21/269183.

Devlin, M., da Silva, E., Petus, C., Wenger, A., Zeh, D., Tracey, D., Alvarez-Romero, J., Brodie, J., 2013. Combining in-situ water quality and remotely sensed data across spatial and temporal scales to measure variability in wet season chlorophyll-a: Great Barrier Reef lagoon (Queensland, Australia). Ecol. Process. 2, 31.

Devlin, M., Petus, C., da Silva, E., Tracey, D., Wolff, N., Waterhouse, J., Brodie, J., 2015. Water quality and river plume monitoring in the Great Barrier Reef: an overview of methods based on ocean colour satellite data. Remote Sens. 7, 12909–12941.

Donovan, M.K., Adam, T.C., Shantz, A.A., Speare, K.E., Munsterman, K.S., Rice, M.M., Burkepile, D.E., 2020. Nitrogen pollution interacts with heat stress to increase coral bleaching across the seascape. Proc. Natl. Acad. Sci., 201915395 https://doi.org/10.1073/pnas.1915395117.

Dormand, J.R., Prince, P.J., 1980. A family of embedded Runge-Kutta formulae. J. Comput. Appl. Math. 6, 19–26.

Duysens, L.N.M., 1956. The flattening of the absorption spectra of suspensions as compared to that of solutions. Biochim. Biophys. Acta 19, 1–12.

Ellis, R., 2018. Dynamic SedNet component model reference guide: update 2017, concepts and algorithms used in source catchments customisation plugin for Great Barrier Reef catchment modelling. Downloaded 12 Jan 2021 from: https://www.publications.qld.gov.au/dataset/dynamic-sednet-reference-guide.

Fabricius, K.E., Logan, M., Weeks, S., Lewis, S., Brodie, J., 2016. Changes in water clarity in response to river discharges on the Great Barrier Reef continental shelf: 2002–2013. Estuar. Coast. Shelf Sci. 173, A1–A15.

Falkowski, P.G., Raven, J.A., 1997. Aquatic Photosynthesis. Blackwell Science.

Furnas, M., 2003. Catchments and corals: terrestrial runoff to the Great Barrier Reefs. In: Tech. Rep. Australian Institute of Marine Science, Queensland, 334 p.

Gillibrand, P.A., Herzfeld, M., 2016. A mass-conserving advection scheme for offline simulation of tracer transport in coastal ocean models. Environ. Model. Softw. 101, 1–16.

Gustafsson, M.S.M., Baird, M.E., Ralph, P.J., 2014. Modelling photoinhibition and bleaching in Scleractinian coral as a function of light, temperature and heterotrophy. Limnol. Oceanogr. 59, 603–622.

Herzfeld, M., 2015. Methods for freshwater riverine input into regional ocean models. Ocean Model 90, 1–15.

Herzfeld, M., Gillibrand, P., 2015. Active open boundary forcing using dual relaxation time-scales in downscaled ocean models. Ocean Model 89, 71–83.

Herzfeld, M., Andrewartha, J., Baird, M., Brinkman, R., Furnas, M., Gillibrand, P., Hemer, M., Joehnk, K., Jones, E., McKinnon, D., Margvelashvili, N., Mongin, M., Oke, P., Rizwi, F., Robson, B., Seaton, S., Skerratt, J., Tonin, H., Wild-Allen, K., 2016. eReefs marine modelling: final report, CSIRO, Hobart, 497 pp. http://www.marine.csiro.au/cem/gbr4/eReefs_Marine_Modelling.pdf.

Hock, K., Wolff, N.H., Ortiz, J.C., Condie, S.A., Anthony, K.R.N., Blackwell, P.G., Mumby, P.J., 2017. Connectivity and systemic resilience of the Great Barrier Reef. PLoS Biol. 11, e2003355.

Hoegh-Guldberg, O., 1999. Climate change, coral bleaching and the future of the world's coral reefs. Mar. Fresh. Res. 50, 839–866.

Hughes, T.P., Kerry, J.T., Connolly, S.R., Baird, A.H., Eakin, M.C., Heron, S.F., Hoey, A.S., Hoogenboom, M.O., Jacobson, M., Liu, G., Pratchett, M.S., Skirving, W., Torda, G., 2018a. Ecological memory modifies the cumulative impact of recurrent climate extremes. Nat. Clim. Change 9, 40–43.

Hughes, T.P., Kerry, J.T., Simpson, T., 2018b. Large-scale bleaching of corals on the Great Barrier Reef. Ecology 22, 501. URL. https://doi.org/10.1002/ecy.2092.

LaJeunesse, T.C., Parkinson, J.E., Gabrielson, P.W., Jeong, H.J., Reimer, J.D., Voolstra, C.R., Santos, S.R., 2018. Systematic revision of Symbiodiniaceae highlights the antiquity and diversity of coral endosymbionts. Curr. Biol. 28 (16), 2570–2580.

Lapointe, B.E., Langton, R., Bedford, B.J., Potts, A.C., Day, O., Hu, C., 2010. Land-based nutrient enrichment of the Buccoo Reef Complex and fringing coral reefs of Tobago, West Indies. Mar. Pollut. Bull. 60, 334–343.

Margvelashvili, N., Herzfeld, M., Rizwi, F., Mongin, M., Baird, M., Jones, E., Schaffelke, B., King, E., Schroeder, T., 2016. Emulator-assisted data assimilation in complex models. Ocean Dyn. 66, 1109–1124.

Maxwell, W.G.H., 1968. Atlas of the Great Barrier Reef. Elsevier, Amsterdam.

McCloskey, G., Baheerathan, R., Dougall, C., Ellis, R., Bennett, F.R., Waters, D., Darr, S., Fentie, B., Hateley, L.R., Askildsen, M., 2021. Modelled estimates of fine sediment and particulate nutrients delivered from the Great Barrier Reef catchments. Mar. Pollut. Bull. 165, 112163.

Mongin, M., Baird, M.E., Tilbrook, B., Matear, R.J., Lenton, A., Herzfeld, M., Wild-Allen, K.A., Skerratt, J., Margvelashvili, N., Robson, B.J., Duarte, C.M., Gustafsson, M.S.M., Ralph, P.J., Steven, A.D.L., 2016. The exposure of the Great Barrier Reef to ocean acidification. Nat. Commun. 7, 10732.

Morris, L.A., Voolstra, C.R., Quigley, K.M., Bourne, D.G., Bay, L.K., 2019. Nutrient availability and metabolism affect the stability of coral-Symbiodiniaceae symbiosis. Trends Microbiol. 27, 678–689.

Muscatine, L., Porter, J.W., 1977. Reef corals: mutualistic symbioses adapted to nutrient-poor environments. BioScience 27, 454–460.

National Academies of Sciences, Engineering and Medicine, 2019. A Research Review of Interventions to Increase the Persistence and Resilience of Coral Reefs. The National Academies Press, Washington, DC.

Oxenford, H.A., Vallès, H., 2016. Transient turbid water mass reduces temperature-induced coral bleaching and mortality in Barbados. PeerJ 4, e2118. https://doi.org/10.7717/peerj.2118.

Packett, R., 2017. Rainfall contributes ~30% of the dissolved inorganic nitrogen exported from a southern Great Barrier Reef river basin. Mar. Pollut. Bull. 121, 16–31.

Rädecker, N., Pogoreutz, C., Gegner, H.M., Cárdenas, A., Roth, F., Bougoure, J., Guagliardo, P., Wild, C., Pernice, M., Raina, J.-B., Meibom, A., Voolstra, C.R., 2021. Heat stress destabilizes symbiotic nutrient cycling in corals. Proc. Natl. Acad. Sci. 118 (5).

Redfield, A.C., Ketchum, B.H., Richards, F.A., 1963. The influence of organisms on the composition of sea-water. In: Hill, N. (Ed.), The Sea, 2nd edition. Wiley, pp. 26–77.

Rocker, M.M., Francis, D.S., Fabricius, K.E., Willis, B.L., Bay, L.K., 2019. Temporal and spatial variation in fatty acid composition in *Acropora tenuis* corals along water quality gradients on the Great Barrier Reef, Australia. Coral Reefs 38, 215–228.

Roelfsema, C., Kovacs, E., Ortiz, J.C., Wolff, N.H., Callaghan, D., Wettle, M., Ronan, M., Hamylton, S.M., Mumby, P.J., Phinn, S., 2018. Coral reef habitat mapping: a combination of object-based image analysis and ecological modelling. Remote Sens. Environ. 208, 27–41.

Rogers, C.S., 1990. Responses of coral reefs and reef organisms to sedimentation. Mar. Ecol. Prog. Ser. 62, 185–202.

Schiller, A., Herzfeld, M., Brinkman, R., Stuart, G., Jan. 2014. Monitoring, predicting and managing one of the seven natural wonders of the world. Bull. Am. Meteor. Soc. 95, 23–30.

Skerratt, J., Mongin, M., Wild-Allen, K.A., Baird, M.E., Robson, B.J., Schaffelke, B., Soja-Woźniak, M., Margvelashvili, N., Davies, C.H., Richardson, A.J., Steven, A.D.L., 2019. Simulated nutrient and plankton dynamics in the Great Barrier Reef (2011–2016). J. Mar. Sys. 192, 51–74.

Skirving, W., Enríquez, S., Hedley, J.D., Dove, S., Eakin, C.M., Mason, R.A.B., Cour, J.L. D.L., Liu, G., Hoegh-Guldberg, O., Strong, A.E., Mumby, P.J., Iglesias-Prieto, R., 2018. Remote sensing of coral bleaching using temperature and light: progress towards an operational algorithm. Remote Sens. 10, 18.

Steven, A.D.L., Baird, M.E., Brinkman, R., Car, N.J., Cox, S.J., Herzfeld, M., Hodge, J., Jones, E., King, E., Margvelashvili, N., Robillot, C., Robson, B., Schroeder, T., Skerratt, J., Tuteja, N., Wild-Allen, K., Yu, J., 2019. An operational information system for managing the Great Barrier Reef: eReefs. J. Oper. Oceanogr. 12 (sup2), S12–S28.

Suggett, D.J., Warner, M.E., Smith, D.J., Davey, P., Hennige, S., Baker, N.R., 2008. Photosynthesis and production of hydrogen peroxide by *Symbiodinium* (Pyrrhophyta) phylotypes with different thermal tolerances. J. Phycol. 44, 948–956.

Sully, S., van Woesik, R., 2020. Turbid reefs moderate coral bleaching under climate-related temperature stress. Glob. Chang. Biol. 26, 1367–1373.

Van Leer, B., 1977. Towards the ultimate conservative difference scheme. IV. A new approach to numerical convection. J. Comp. Phys. 23, 276–299.

Waterhouse, J., Schaffelke, B., Bartley, R., Eberhard, R., Brodie, J., Star, M., Thorburn, P., Rolfe, J., Ronan, M., Taylor, B., Kroon, F., 2017. 2017 Scientific Consensus Statement: land use impacts on the Great Barrier Reef water quality and ecosystem condition, Chapter 5: overview of key findings, management implications and knowledge gaps. In: Tech. Rep. State of Queensland.

Waterhouse, J., Henry, N., Mitchell, C., Smith, R., Thomson, B., Carruthers, C., Bennett, J., Brodie, J., McCosker, K., Northey, A., Poggio, M., Moravek, T., Gordon, B., Orr, G., Silburn, M., Shaw, M., Bickle, M., Ronan, M., Turner, R., Waters, D., Tindall, D., Trevithick, R., Ryan, T., VanderGragt, M., Houlden, B., Robillot, C., 2018. Paddock to reef integrated monitoring, modelling and reporting (paddock to reef) program design, 2018–2022. downloaded on 12 Jan 2021 from: https://www.reefplan.qld.gov.au/data/assets/pdf_file/0026/47249/paddock-to-reef-program-design.pdf.

Waters, D., Carroll, C., Ellis, R., Hateley, L., McCloskey, J., Packett, R., Dougall, C., Fentie, B., 2014. Modelling reductions of pollutant loads due to improved management practices in the Great Barrier Reef catchments — whole of GBR. Tech. rep., Queensland Department of Natural Resources and Mines, Toowoomba, Queensland. Downloaded on 12 Jan 2021 from: https://www.reefplan.qld.gov.au/data/assets/pdf_file/0027/46098/great-barrier-reef-catchment-modelling-report.pdf.

Wiedenmann, J., D'Angelo, C., Smith, E.G., Hunt, A.N., Legiret, F.-E., Postle, A.D., Achterberg, E.P., 2013. Nutrient enrichment can increase the susceptibility of reef corals to bleaching. Nat. Clim. Chang. 3, 160–164.

Wolff, N.H., da Silva, E.T., Devlin, M., Anthony, K.R.N., Lewis, S., Tonin, H., Brinkman, R., Mumby, P.J., 2018. Contribution of individual rivers to Great Barrier Reef nitrogen exposure with implications for management prioritization. Mar. Pollut. Bull. 133, 30–43.

Wooldridge, S.A., 2009. Water quality and coral bleaching thresholds: Formalising the linkage for the inshore reefs of the Great Barrier Reef, Australia. Mar. Pollut. Bull. 58, 745–751.

Wooldridge, S.A., 2020. Excess seawater nutrients, enlarged algal symbiont densities and bleaching sensitive reef locations: 1. Identifying thresholds of concern for the Great Barrier Reef, Australia. Mar. Pollut. Bull. 152, 107667.

Yonge, C.M., 1930. A Year on the Great Barrier Reef: The Story of Corals and of the Greatest of Their Creations. Putham, London.